Analysis of the North Anatolian Fault Zone in Central Pontides (Northern Turkey): insight for geometries and kinematics of deformation structures in a transpressional zone

Alessandro Ellero[a], Giuseppe Ottria[a], Michele Marroni[ab], Luca Pandolfi[ab], M. Cemal Göncüoğlu[c]

[a] Istituto di Geoscienze e Georisorse, CNR, 56124, Pisa, Italy

[b] Dipartimento di Scienze della Terra, Università di Pisa, 56126, Pisa, Italy

[c] Department of Geological Engineering, Middle East Technical University, 06531 Ankara, Turkey

ABSTRACT

The western part of the North Anatolian Fault Zone at the southern boundary of the Central Pontides in Turkey, was investigated in the Kursunlu-Arac area by means of a geological-structural field study. In this area the North Anatolian Fault Zone results in a transpressional deformation zone that extends between two master faults striking parallel to the main shear direction. The main systems of structures identified in the deformation zone appear to be oriented parallel to the directions predicted by Riedel theoretical model. Nevertheless, the strain partitioning is more complicated than predicted by theory. The structural analysis suggests a polyphase deformation characterized by a steady component of trascurrence associated to alternance of compression or extension. Along each of theoretical directions the combination of double vergence structures can be observed, with thrust surfaces and folds rooted in high-angle shear zones, according to flower-type geometries. The discrepancies of directions, kinematics and geometries from theoretical models are due to transpressive and / or transtensive nature of the deformation. According to the outcropping observed structures, we propose a conceptual model for the North Anatolian Fault Zone, interpreting it as a crustal-scale positive flower structure.

1. Introduction

Regional scale strike-slip faults are widespread tectonic features of the earth's crust that accommodate large-scale motion of lithospheric plates (Wilson, 1965). These structures

are characterized by steeply dipping, straight development and prominent geomorphic features (Cunningham and Mann, 2007 with references).

The strike-slip deformation often is not concentrated along a single fault, but is distributed along interlinked systems of faults and shear zones bounded blocks, according to a complex strain-partitioning model at various scales (Oldow et al. 1990; Tikoff and Teyssier 1994; Jones and Tanner 1995; Dewey et al. 1998).

Because the strike-slip zones typically developed in mechanically heterogeneous crust, pre-existing tectonic features as older suture zones can be reactivated (White et al., 1986; Holdsworth et al., 1997).

The North Anatolian Fault (NAF) (Ketin 1948, 1957; Allen 1969; Ambraseys 1970; Şengor 1979; Barka 1992) is a major continental dextral strike-slip fault, which extends for about 1400 km from the Karliova basin in the east to the Aegean Sea in the west (Taymaz et al. 1991; Kocyigit et al. 2001; Yilmaz et al. 2002; Sengor et al. 2003).

As the NAF is one of the world's major active fault system, the discussion about the NAF time-space evolution attracted the most attention. Therefore a huge number of studies about paleoseismology, seismicity, paleomagnetism, GPS measurements, geophysical modelling, geodynamics and global tectonics regarding the NAF and Anatolian plate has been produced and published. In comparison the geological studies about geometry and kinematics of the tectonic structures associated to the NAF are few (Andrieux et al., 1995; Bozkurt and Kocyigit, 1996; Sunal & Tüysüz, 2002; Ozden et al., 2008) and mostly concentrated in the western part of the NAF itself (Neugebauer, 1995; Yaltırak et al., 1998; Okay et al., 1999, 2000; Yaltırak & Alpar, 2002; Yiğitibaş et al., 2004; Ozden et al., 2008).

In this contribution we present the results of a geological-structural field study carried out along a transect crossing the central part of the NAF at the southern boundary of the Central Pontides in the Kursunlu-Arac area. The characterization of the geometries and kinematics of the studied tectonic structures, suggesting the occurrence of main transpressional systems, indicates that strain partitioning played an important role in the deformation evolution of the NAF. The described structures are interpreted inside a regional crustal setting, and their possible relationships with inherited tectonic structures are commented.

2. The North Anatolian Fault Zone

The NAF belongs to a complex fault system bounding the Anatolian plateau, along a continental collisional zone where the Arabian Plate collides with the Eurasian Plate. Several models have been proposed for this collisional zone suggesting continental subduction (Rotstein and Kafka, 1982), lithospheric thickening (Dewey et al., 1986), lithospheric delamination (Pearce et al., 1990), or else convergence accommodation between Arabian and Eurasian plates by means of the westward movement escape (Mc Kenzie, 1976; Sengor & Kidd, 1979; Jackson & Mc Kenzie, 1988) and/or the counterclockwise rotation of the Anatolian block (Rotstein, 1984; Reilinger et al., 1997; Piper et al., 2010). The westward movement of the Anatolian block is made possible by the release along two regional scale strike-slip zones corresponding to the NAF itself, which coincides with the northern limit of the Anatolian block, and the left-lateral East Anatolian Fault (EAF), corresponding to the eastern boundary of the Anatolian block (Fig. 1). Likewise the geodynamic context, the nature of these two main faults is discussed, being interpreted in some cases as transform faults, that is as true plate boundaries, and then extended to the lithospheric mantle (Sengor, 1979; Barka 1996; Piper 1997; Stein 1997; Hubert Ferrari et al., 2002; Biryol et al., 2010), or as "indent-linked strike-slip faults" (Woodcock, 1986), that is crustal faults which enable the process of tectonic escape between the several crustal blocks interposed between Arabian and Eurasian plates (Dewey & Sengor, 1979; Sengor et al., 1985; Sylvester, 1988; Sengor, 1990).

The NAF is a seismically active structure, with the most destructive earthquakes that have generally a relatively shallow focal depth, within the first 10 km of the crust. However deep hypocentral depths (10-30 km) are reported, suggesting a lower crustal depth for the fault (Turkelli et al., 2003). Additional information about possible extension at depth of the NAF, are provided by geochemical studies of thermal fluids discharged along the fault, that partly seems to be mantle-derived suggesting a lithospheric nature for the NAF (Gulec et al., 2002; de Leeuw et al., 2010) and the EAF (Italiano et al., 2013).

NAF and EAF faults cross at the Karliova triple junction. Actually the North Anatolian Fault does not terminate at the Karliova triple junction but extends for some kilometres (50 km) towards south-east as the Varto fault system (Turkelli et al., 2003; Hubert-Ferrari et al., 2009).

Referring to its direction along its trace, the NAF can be separated into three main segments: an eastern part trending N110-120°E, a central northern convex part, and a

western part with N75°E trend (Barka, 1992). The western segment, which lies in the Marmara Sea region, splays into two branches that continue as separate northern and southern strands to the east of the Marmara Sea (Fig. 1) (Le Pichon et al., 2001; 2003).

GPS measurements (Kiratzi, 1993; Reilinger et al., 1997; McClusky et al., 2000; Hubert-Ferrari et al., 2002; Meade et al. 2002) indicated that the present-day right-lateral displacement on the NAF is between 16 and 30±2mm/year. Reilinger et al. (2006) calculated a displacement rate of 24.2 mm/year in the Bolu area.

As the other major strike-slip faults worldwide (e.g. San Andreas Fault), the North Anatolian Fault is not a single plane but a fault zone, the North Anatolian Fault Zone (NAFZ), that can be as much as 100 km wide, characterized by a series of subparallel strike-slip faults (e.g. Ambraseys, 1970; Barka, 1992). The geometries along NAFZ determined the formation of releasing and restraining bends. In correspondence of releasing bends several pull-apart basins have developed (e.g. Barka et al., 2000; Sengor et al., 2005). These basins are important features since they contain valuable information on the age and kinematic evolution of the NAFZ.

The timing of the NAFZ formation is controversial. Based on the age of fault-related basin deposits it is supposed to be active since Late Miocene (11 Ma) (Sengor et al., 2005 and references) starting from its easternmost part, the triple junction with the EAF. The westward time-space propagation of the NAFZ is accepted by many authors. From Central Anatolia to Marmara region and Aegean Sea the fault zone became active in Late Miocene-early Pliocene, early-middle Pliocene and Pleistocene, respectively (Hubert-Ferrari et al., 2002, 2003 and references). However, other studies suggested as age of initiation of the NAFZ the Early Pliocene (e.g. Barka, 1992; Kocyigit et al. 2001). Also the activation age of the NAFZ in the Marmara region is not univocal, ranging from 5 Ma (Armijo et al., 1999; Hubert-Ferrari et al., 2003) to 3.5 Ma (Sengor et al., 2005). Nevertheless, western segments of the NAFZ in the Marmara region have been documented as active faults during the late Oligocene (Zattin et al., 2005, 2010) and even earlier (~ 57 Ma; latest Paleocene–Early Eocene) resulting from K-Ar dating of fault rocks (Uysal et al., 2006).

The total offset of the NAFZ is a debated issue too. The suggested cumulative displacements range from few kilometres to more than 300 km (see the review in Herece and Akay, 2003). However the documented offset of about 85 km (Westaway 1994; Armijo et al. 1999; Barka et al. 2000) seems in good agreement with the estimations measured on more reliable markers (see the discussion in Sengor et al., 2005).

3. Geological setting

We focused our study in an area across the western branch of the NAFZ, showing a N75°E trend, at west of the culmination point of the convex-northwards arc of the NAFZ (Fig. 1). In this sector the NAFZ roughly coincides with the Intra-Pontide suture zone (Sengor and Yilmaz, 1981; Andrieux et al., 1995), the tectonic contact zone between the Sakarya and Istanbul-Zonguldak terranes. This area corresponds to the central part of the Pontide orogenic belt (Central Pontides; Okay et al., 2006), between the Izmir-Ankara-Erzican suture and the Black Sea (fig. 2). At a regional scale the Istanbul-Zonguldak terrane is made up of: i) Late Proterozoic crystalline basement and overlying Ordovician-Carboniferous trasgressive succession which suffered deformation during the Carboniferous Hercynian orogeny (e.g. Görür et al., 1997) which did not developed metamorphism; ii) Triassic rocks, unconformably overlying the Paleozoic succession, characterized by a flysch-like sequence of sandstones and shales marking the onset of the Late Triassic Cimmeride deformation; iii) Upper Cretaceous-Paleocene carbonate and clastic deposits intercalated by Cretaceous andesitic volcanic rocks. In particular Upper Jurassic-Lower Cretaceous platform carbonates unconformably overlies the Triassic as well as the Palaeozoic rocks and are in turn succeeded by a thick succession of conglomerates, sandstones and shales with minor limestones evolving in age up to the early Eocene (Tüysüz, 1999).

The Sakarya terrane is instead represented by high-grade (amphibolite to granulite facies) Variscan (Carboniferous) metamorphic rocks (Paleozoic gneiss, amphibolites and marbles). However the distinctive geological feature of the Sakarya terrane is the Triassic subduction-accretion complex (Karakaya complex) strongly deformed and metamorphosed by the Cimmeride tectonics (Okay and Göncüoğlu, 2004; Okay et al., 2006; Sayit & Goncuoglu, 2013). In the Central Pontides granitic rocks were intruded into the basement during the Early to Middle Jurassic (Yılmaz and Boztuğ, 1986) and the Karakaya complex was unconformably overlain by Middle Jurassic continental clastic rocks evolving to Upper Jurassic-Lower Cretaceous limestone sequence, which can be followed throughout the Sakarya Zone (Altiner et al. 1991). The limestones are unconformably overlain by Upper Cretaceous-Paleocene succession made up of clastic rocks (deep sea sandstones and shales) and pelagic limestones with a Upper Cretaceous intercalation of volcanic rocks. The andesitic volcanism is related to the northward subduction of the Izmir-Ankara-Erzincan ocean (Okay & Tüysüz, 1999). The collision between the Central Pontides and

the Kirschir Massif of the Anatolide-Tauride Block began in the Late Paleocene (e.g. Kaymakci et al., 2003) and was marked by the Izmir-Ankara-Erzincan suture zone representing the former position of the subduction zone of a branch of the Neo-Tethys ocean (Şengör and Yılmaz, 1981).

On the contrary, the Intra-Pontide suture zone originated from the continental collision and accretion between the Istanbul-Zonguldak and Sakarya terranes which occurred during the early Late Cretaceous in the Central Pontides (Cenomanian-Turonian; Tüysüz, 1999). The Intra-Pontide suture zone is represented by Middle Jurassic oceanic assemblages and Late Cretaceous melange complexes composed of large bodies of ultramafic and volcano-sedimentary rocks, basic lavas, radiolarian cherts and allochthonous blocks of Jurassic-Early Cretaceous limestones (Goncuoglu et al., 2008; 2012). The units of the Intra-Pontide suture zone belong to an imbricated structural stacking, resulting interposed between the overthrust of the Istanbul-Zonguldak units, at the top, and the Sakarya units at the bottom (Yılmaz et al., 1995; Robertson & Ustaömer, 2004; Goncuoglu et al., 2008; Catanzariti et al., 2013 in press).

Following the collision, the units derived from Istanbul-Zonguldak, Intra-Pontide and Sakarya zones were deformed further developing a thin-skinned foreland fold-and-thrust belt during the Paleocene-Eocene age (Sunal & Tüysüz, 2002). The relationships among these units are sealed by Middle Eocene sedimentary deposits (conglomerates and sandstones) which are deformed due to the activity of the NAFZ as well as the Neogene formations that deposited in the pull-a-part basins developed along the NAFZ (e.g. Andrieux et al., 1995).

4. The Kursunlu-Arac area

The zone where the geological-structural study has been performed corresponds to an about 1600 km^2 wide area north to Kursunlu roughly limited to the north by the Arac valley (Fig.2b, 3). In the study area the three terranes that characterized the Central Pontides at a regional scale are represented.

The Istanbul-Zonguldak terrane is represented only by Devonian platform carbonates and minor Upper Jurassic-Lower Cretaceous limestones.

The Sakarya terrane is represented by Upper Jurassic-Lower Cretaceous succession, formed by limestones and dolomites, which is overlain by the Tarakly Flysch. The latter is formed by a thick succession mainly characterized by turbidites, consisting of arenites and

siltites showing a thickening and coarsening upward evolution, and slide-block in shaly-matrix lithofacies. The Tarakly Flysch has been dated by nannofossil assemblages to the Early Maastrichtian-Middle Paleocene interval and interpreted as foredeep deposits (Catanzariti et al., 2013; in press).

Interposed between Istanbul-Zonguldak and Sakarya terranes, the Intra-Pontide suture zone is formed by three tectonic units, respectively from top to bottom: i) the Ayli Dag Unit (Göncüoğlu et al., 2012), represented by an ophiolite sequence consisting of peridotites, layered gabbros basalts and radiolarian cherts, the latter dated to the Middle Jurassic. This unit has been interpreted as witness of a Middle Jurassic back-arc spreading within the Intra-Pontide oceanic basin, which in turn indicates an intra-oceanic subduction during the same time interval (Göncüoğlu et al., 2012); ii) the Arkotdag Melange Unit (Tokay, 1973; Göncüoğlu et al., 2013 in press), represented by a chaotic succession with slide blocks of sedimentary, metamorphic and ophiolite rocks ranging in size from few meters to one-two hundreds square meters, enclosed in a sedimentary matrix consisting of pebbly mudstones, pebbly sandstones and coarse-grained arenites; iii) Low Grade Metamorphic Unit (Goncuoglu et al., 2012), consisting of a thick succession of actinolite-bearing metabasites, metacarbonates, metapelites and metarenites.

The study area is also characterized by the post-collisional Eocene deposits resulting as filling of the Karabuk-Kastamonu inter-mountain basin. In particular, Hippolyte et al. (2010) documented that the deposition started in the Early Eocene (NP12 Nannoplankton zone) and stopped in the Middle Eocene (NP17 Nannoplankton zone) also basing from data collected in the Kursunlu-Arac area which encompass the complete time interval. The lowermost formation of the Karabuk-Kastamonu basin succession is formed by shallow-marine deposits, comprising mainly clastic rocks and argillaceous carbonates unconformably overlying the rocks of the Istanbul-Zonguldak terrane (Safranbolu Formation).

The stratigraphic sequence has developed upward with a thick succession of conglomerates/sandstones/siltstones and massive shales, interpreted as fluvio-deltaic deposits (Özcan et al., 2007), and representing the Eocene lithofacies more extensively cropping out in the sector between Bayramoren and Bahcecik. At the northeastern boundary of the study area the Middle Eocene is characterized by volcaniclastics and lavas spanning the whole compositional range from basalts to rhyolites (Keskin et al., 2008).

At the southwestern limit of the study area shown in the Fig. 2b, east of Eskipazar, the Miocene volcanic rocks of the Galatia Province (Tankut et al., 1998) crops out involved inside the NAFZ fault system. The southeastern limit of the study area, nearby the Yesildumlupinar village (Fig. 3a), includes a small patch of the Cerkes-Kursunlu Neogene basin, characterized by an Upper Miocene-Pliocene fluvio-lacustrine succession (Sengor et al., 2005 and references).

In the Kursunlu-Arac area the relationships among the different units belonging to the three main tectonostratigraphic zones are represented by low-angle tectonic contacts, partially inherited from the Cretaceous subduction and continent collision evolution between Sakarya and Istanbul-Zonguldak terranes. The low-angle contacts were sealed by the mainly clastic and volcanic deposits of the Eocene basins and after resumed by high-angle faults connected with the Miocene strike-slip tectonics related to the NAFZ. The study area lies, indeed, between two main tectonic lineaments of the NAFZ system: the Arac Fault Zone (AFZ), to the north, and the Bayramoren Fault Zone (BFZ), to the south. North AFZ the Karabuk-Kastamonu Eocene basin develops (Tuysuz, 1999; Hippolyte et al., 2010), overlying the Istanbul-Zonguldak terrane (Fig. 2). North of Bahcecik village, a slice of Istanbul-Zonguldak rocks is involved by the high-angle fault system of the AFZ (Fig.3).

Along the southern limit of the study area, the BFZ coincides with the main lineament of the NAFZ (Fig.3) that defines the morphotectonic structure of the Ilgaz Range (Yìldirim, et al. 2011). South BFZ tectonic slices belonging to the Intra-Pontide Suture Zone occur, overtrhusting along low-angle tectonic contacts the Sakarya units. These relationships between the two terranes were sealed by the Miocene-Pliocene deposits accumulated in the sedimentary basins connected to the NAFZ activity (i:e. Cerkes-Kursunlu basin).

Between the two main AFZ and BFZ lineaments, we can identify the Boyali area, where the tectonic units belonging to the three tectonostratigraphic terranes crop out being juxtaposed to each other along low-angle tectonic contacts then cut by high-angle strike-slip faults. The relationships along the low-angle contacts were unconformably sealed by the Eocene deposits (Fig. 2 and 3).

Below, the structures that characterize the BFZ, the AFZ and the Boyali area will be described in detail.

4.1 The Bayramoren Fault Zone

The BFZ corresponds to a shear zone elongated in the WSW-ESE direction with a variable width ranging from about 2 km up to 8 km (Fig. 3). The main structure is a master fault represented by a high-angle dextral strike-slip fault developing along the morphological high of the Ilgaz Range, coinciding with the belt formed by Upper Jurassic-Early Cretaceous limestones of the Sakarya terrane (Fig. 3). Subparallel secondary high-angle strike-slip faults, associated with the major fault, are well observable at the outcrop scale. The statistical analysis of fault trends shows that the overall directions of these secondary faults differ slightly from the map direction of the BFZ clustering around the NE-SW (N45E) direction as S1 fault system (Fig. 4). The data collected along the BFZ point to the occurrence of a second S2 fault system with a trend distribution around the NW-SE direction.

Low-angle thrusts that root into the high-angle faults are associated with both S1 and S2 fault systems; kilometric size fault-bounded blocks are therefore defined along the BFZ being formed by rocks belonging to Jurassic carbonate succession, units of the Intra-Pontide suture zone and Eocene deposits (Fig. 5).

Both S1 and S2 fault systems are characterized by a mainly dextral strike-slip kinematics (Fig. 6a) compatible with a strike-slip paleostress tensor displaying sub-horizontal maximum compression σ1 axis and minimum compression σ3 axis respectively directed NNW-SSE (13/330) and ENE-WSW (09/062) (Fig. 4c).

South of Bayramoren village, the master fault crosses obliquely the fault-bounded block made up of Jurassic limestones, identifying a positive flower structure characterized by low-angle shear planes, verging both to the south and to the north, rooting into the main fault (Fig. 6b). A similar flower structure developed also at the map scale, causing the northward overthrusting of the Arkotdag melange unit on the Tarakli Flysch and the southward overthrusting of the Jurassic limestones of the Sakarya terrane on the Arkotdag melange (cross-section C-C’ in Fig. 3b).

At the boundary between the Jurassic limestones and the Arkotdag melange, the BFZ master fault comprises broad zones, hundreds of metres wide, characterized by cataclasites, breccias and phyllonites documenting that the fault zone has undergone intense and complex deformation (Fig. 3).

The analysis of striated slip surfaces indicates that the low-angle thrusts are characterized by an oblique reverse kinematics (Fig. 6c).

Folding appears frequently associated with the low-angle thrust planes, being both north-verging and south-verging hanging-wall anticlines the prominent fold structures. An example of these hanging-wall anticlines at the outcrop scale is reported in Fig. 6d. The direction of the fold axes is sub-parallel to the direction of the thrust and the axial surfaces are moderately to steeply inclined planes.

4.2 The Arac Fault Zone

The Arac Fault Zone (AFZ) is a SW-NE trending main fault zone belonging to the NAFZ system that extends for more than 300 km from the Almacik Mts., at SW, to Kastamonu at NE (Elmas & Yiğitbaş, 2001; Aksay et al., 2002; Uğuz et al., 2002).

In the study area the AFZ represents the southern boundary of the Karabuk-Kastamonu Eocene basin and appears displaced by a NNW-SSE trending fault system. The main fault shows also a clear geomorphic expression corresponding to the steep scarp between the Arac plain and the Dikmen Dagi mountains (Fig. 7).

Actually, also the AFZ is a brittle shear zone composed by an high-angle S1 fault system mainly directed WSW-ENE (Fig. 8). Besides the main S1 fault system, the statistical analysis gives other two peaks at about N110 and N20, representing two much less apparent fault systems respectively directed WNW-ESE (S2 fault system) and NNE-SSW (S3 fault system) (Fig. 8). On the whole, the three fault systems are composed by mainly high-angle strike-slip and oblique faults; in particular the S1 fault system is characterized by a dextral kinematic, whereas the S3 fault system displays mainly sinistral component. The fault slip data inversion for the strike-slip faults of S1 and S3 systems allowed to determine a paleostress tensor characterized by a sub-vertical intermediate compression σ2 axis and horizontal maximum compression σ1 and minimum compression σ3 axes respectively directed WNW-ESE (10/301) and NNE-SSW (01/031) (Fig. 8c).

In the western sector of the study area the AFZ is characterized by an evident gentle restraining bend where high-angle faults identify fault-bounded blocks of Paleozoic and Mesozoic limestones belonging to the Istanbul-Zonguldak terrane, juxtaposed to blocks of Tarakli Flysch (Sakarya terrane). On plan view, the restraining bend is formed by NE-SW elongated trapezoid-shaped blocks which are defined by faults with a variable spacing of approximately 1-3 km (Fig. 3a).

Low-angle thrust planes showing south vergence are associated with the high-angle faults; these structural features are particularly noticeable in the Tarakli Flysch (cross-

section A-A' in Fig. 3b). In fact, the intensity and style of deformation within the fault-bounded blocks are not completely homogeneous. The Tarakli Flysch block adjacent to the AFZ main fault shows a remarkable assemblage of low-angle thrusts and associated folds that contrasts with the greater structural simplicity of the blocks formed by Devonian and Mesozoic limestones.

The main fault juxtaposing the Eocene deposits with the Tarakli Flysch crops out along a road cut in the western part of the study area along the NW-SE stretch of the Akcay River (Fig. 3, 7 and 9). The AFZ main shear zone is formed by a 60-70 m wide fault zone characterized by a central part verticalized at the main fault plane where low-angle thrusts are rooted. These thrust planes show an opposite vergence and are characterized by a complex kinematics. Observing the outcrop along sections cut in the xz-plane of finite strain ellipsoid, we detected S-C type brittle structures suggesting a compressional kinematics (Fig. 9a and c). Observing the same structures on the xy-plane of finite strain ellipsoid, a dextral strike-slip component of movement is instead prominent (Fig. 9b). Therefore these S-C structures formed as a result of strain partitioning within a dextral transpressional tectonic regime.

The AFZ main fault crops out also northeastward, south of Arac, where it is clearly visible, cutting the Eocene deposits (Fig. 10).

4.3 The Boyali Area

The Boyali area, between the AFZ at north and the BFZ at south, displays units from Sakarya terrane and Intra-Pontide suture zone. The tectonic stack was achieved after the Upper Cretaceous collision when the units involved in the suture zone overthrusted the Upper Cretaceous-Paleocene foredeep deposits of the Tarakli Flysch (Sakarya terrane).

In order to investigate the post-Paleocene deformation history, the structural analysis has been specifically performed on the Tarakli Flysch. Besides the low-angle contacts, the first deformation phase (D1) is represented by rootless isoclinal folds with steeply plunging fold axes (Fig. 11a) showing a dispersion of axis directions. However, the most evident deformation is due to the following phases clearly linked to a tectonics with a strike-slip component. The dominant structures are represented by high-angle faults (Fig.11b) that can be grouped into three prevailing systems (Fig. 12b): the S1 system is that with faults parallel to the directions of the NAFZ system, i.e. approximately E-W; the S2 system has

faults with a roughly NW-SE direction; the S3 system is characterized by faults with directions ranging from NNW-SSE to NNE-SSW.

Inside the Boyali area the dominant fault system is the S3 fault system, composed by high-angle strike-slip faults characterized by a mainly sinistral kinematics. The faults belonging to S1 and S2 systems are instead characterized by a mainly dextral kinematics (Fig. 11c). During field structural analysis, no clear cross-cutting relationship has been detected, therefore the conjugate nature of the three fault systems seems likely.

Overall, the faults display similar features at the outcrop scale: they are high-angle strike-slip faults that frequently have been reactivated as normal faults. In these cases the horizontal-oblique striations are overprinted by sub-vertical dip-slip slickenlines on a single fault surface (Fig. 11d). Therefore, even if the three main fault systems can be referred to a single brittle tectonic event, we should admit the occurrence of a later tectonic phase that reactivated the previous fault structures.

The field work has highlighted that low-angle fault surfaces, characterized by inverse-oblique kinematics, are coupled to the high-angle faults. The thrust faults show a double vergence and cause the development of overthrusting, duplex structures and shear zones with S-C type brittle structures (Fig. 11e). Bedding/foliation is deformed by folds with variable geometry, generally low-angle axial planes and axes directed parallel to the high-angle fault trends to which are associated. On the whole, the structure at the outcrop scale can be therefore described as a flower structure characterized by folds linked to the development of double-verging thrust systems that root in sub-vertical fault planes (Fig. 11f).

5. Discussion

5.1 The transpressional fault systems

The main tectonic feature of the study area is the NAFZ which actually consists in a wide shear zone between two parallel master faults, the AFZ and the BFZ (Fig. 2 and 3). The most evident deformation is linked to the activity of these two master faults that transposed the previous structures.

The Boyali area between the two master faults represents a deformation zone that separates two crustal blocks, a northern block, north of the AFZ, from a southern block, south the BFZ.

The whole study area between Kursunlu and Arac, is characterized by three main structure systems, with similar geometries but differing in the direction (S1, S2 and S3 systems). These systems are significant throughout the study area, even if widespread unevenly. In fact, along the southern boundary of the study area corresponding to the BFZ only S1 and S2 systems are observed predominantly, whereas the S3 system is less pervasive. Instead, S1, S2 and S3 systems are present together along the northern boundary corresponding to the AFZ and in the Boyali area. All three systems are formed by high-angle strike-slip faults associated with low-angle thrust surfaces and folds describing flower-like geometries. While the high-angle faults have displaced and transposed the previous structures, the low-angle shear zones often have reactivated the original tectonic contacts between the different units (Fig. 3).

The S1 system is overall characterized by dextral strike-slip faults with directions coinciding with the map trend of the NAFZ of which AFZ and BFZ represent the main structures in the study area (Fig. 2 and 3). The S2 system is instead constituted by WNW-ESE-directed dextral strike-slip faults. Finally, the S3 system is represented by sinistral strike-slip faults showing a direction ranging from NNW-SSE to NNE-SSW.

The statistical analysis of fault trend, compared with the directions of low-angle thrusts and associated fold axes, points to a substantial parallelism inside each of three systems (Fig. 13). This overall kinematic-geometric arrangement is compatible with a transpressional tectonic regime featuring the study area. The flower structures are widespread structures at the mesoscale documenting the development of a transpressional deformation which is partitioned between high-angle strike-slip faults and lower angle reverse faults (e.g. Wilcox et al, 1973; Sanderson and Marchini, 1984; Tikoff and Teyssier, 1994). Within this context, strike-slip faults are not offset by the thrusts and vice-versa, this supporting that thrusts are genetically related to the sub-parallel strike-slip faults.

The field observations about crosscutting relationships among the three structure systems point to an absence of clear superposition evidences, thus suggesting that these systems developed at a similar time or at least were active during the same tectonic event.

In particular, their substantial contemporaneity could be interpreted as synthetic and antithetic systems, respectively the S2 system and the S3 system, linked to a main dextral transpressional S1 system represented by AFZ and BFZ shear zones (Fig. 14).

5.2 Comparison with theoretical models

Referring to theoretical models of pure strike-slip tectonics (wrench tectonics) (e.g. Wilcox et al., 1973), the faults belonging to S1, S2 and S3 systems can be interpreted as the main strike-slip faults parallel to the main shear direction or principal displacement zone (PDZ in Fig. 14), the synthetic Riedel shears (R in Fig. 14) and the antithetic shears (R' in Fig. 14), respectively.

In the classical Riedel model experiments, the synthetic faults formed at low angles of about 12°-20° to the main shear direction (Tchalenko, 1970; Naylor et al., 1986), whereas the antithetic faults form high angles, between 70° and 90°, with the main shear direction (Tchalenko, 1970; Wilcox et al., 1973). In Fig. 14 each fault detected inside the Boyali area has been tentatively referred to the fault systems predicted by the theoretical model. What is observed is a general good correspondence with the theoretical model; the angular deviations from the expected values can be interpreted as due to transpressional rather than pure strike-slip regime. Indeed, in transpression the Riedel faults are formed at a higher angle to the shear direction (Naylor et al., 1986; Casas et al., 2001). In particular, the Riedel synthetic faults in transpressional models form angles to the main shear direction with mean values of about 37° which can reach a maximum of 60° (Naylor et al., 1986). In the study area the main strike-slip faults parallel to the main shear direction are oriented N70, while the faults interpreted as belonging to the Riedel synthetic fault system form an angle of approximately 35°-40°, in perfect agreement with what is predicted by the theoretical models for transpression (Naylor et al., 1986).

The antithetic faults show a greater direction variability, with angles to the main shear direction ranging from 90° to 120°. The model experiments predict that antithetic shears striking at approximately 80° formed nearly coevally with the R shears during the early stages of deformation (Dooley & Schreurs, 2012 with references). Because of their large angle to the shear direction, the R' shears rapidly became inactive and were rotated clockwise in dextral shear zones.

Some uncertainties concern a few faults attributed to the main strike-slip faults that actually may belong to a further system of synthetic faults, namely the P shears, forming angles up to 40° to the main shear direction (Wilcox et al., 1973).

Analogue models of transpressional systems showed that low angle thrusting develops parallel to the main shear direction (Casas et al., 2001). The development of thrust faults associated with high angle strike-slip faults is connected to the α angle that the maximum

stress axis σ_1 form with the main shear direction. When this angle ranges between 15°-20° the strike-slip structures are dominant compared to the thrust surfaces (Casas et al., 2001; Schreurs & Colletta, 2003).

When these angle values are exceeded, thrust faults become more important and the transpression is thrust-dominated. For values of $\alpha = 30°$ the transpressional experiments provide for the formation of symmetric pop-up structures bounded by conjugate fault zones associated with a symmetric uplift (Casas et al., 2001).

In the study area, the structural situation is more complex, since low angle thrust surfaces, showing double vergence, are associated with all the three recognized high-angle fault systems (S1, S2 and S3); these thrust faults strike parallel to the different fault systems. The situation is made even more complex being present older thrusts which have been in some cases deformed and in other cases reactivated by the later transpressional tectonics.

Therefore, unlike than expected by analogue models of transpressional systems, within a zone subject to transpression, the deformation is distributed in a more complex way. While the models developed flower structures with strikes parallel to the main shear direction, the study area is characterized by symmetric and double-verging structures with different strikes which roughly correspond to the directions of main, synthetic and antithetic shears provided by the models.

Folds seem also to develop with different trending, being the axis directions parallel to the three fault systems S1, S2 and S3 (Fig. 13).

The Riedel model for simple shear provides for the development of normal faults with directions parallel to σ_1 (Fig.14). Although such structures have not been observed in the study area, an extensional component of deformation seems to set itself on faults belonging to the three identified systems, often as the last event of a polyphase kinematics (Fig.11d).

5.3 The NAFZ evolution as a crustal scale flower structure

In the Kursunlu-Arac area, the younger deposits affected by transpression along the NAFZ show a Pliocene age (Fig. 3). Several authors admit the NAFZ rejuvenation from east to west. In the eastern branches the fault appears to be active from the Late Miocene (Hubert-Ferrari et al., 2002, 2003 and references), while in the western branches, in the Marmara Sea region, the fault begins to be active in the Pleistocene (Le Pichon et al.,

2001). In the study area, the age of NAFZ activity is placed in the middle Pliocene (Sengor et al., 2005). These ages are estimated considering the sedimentary basins along the NAFZ as basins related to deformation along the fault and then as syn-transcurrent basins (e.g. Sengor et al., 2005). The age of the NAFZ activity in each sector is therefore inferred from the dating of deposits of the corresponding basins.

A possible alternative is to consider the development of these basins as only one of the several NAFZ activity stages. The polyphase kinematics observed along the fault systems is consistent with the suggested perspective and attests a deformation in which inverse, strike-slip and normal faulting alternate and interfere (Fig. 11d).

In this case, the age of NAFZ tectonics may also be older. An older age of the activity along directions parallel or coincident with the NAFZ is in agreement with the hypotheses of Ylmaz et al. (1993) and Zattin et al. (2005, 2010).

In this context, the Eocene deposits outcropping inside restraining bend belonging to the BFZ system, north and northeast of Bayramoren (Fig. 3a), could be reconsidered in a new perspective. The massive conglomerates and sandstones would have accumulated as sedimentary fill of a pull-apart basin during a transtensional phase, contemporaneous to the volcanic activity that characterizes the Late Eocene succession in the study area. This suggestion needs further investigations and studies concerning dating, structural evolution as well as depositional characters of these deposits.

Leaving aside the discussion about the inception of its activity, geomorphic and structural evidences show that the NAFZ has been active during the Quaternary and the historical seismicity suggests that several brittle structures are still active (Fig. 15a). The more intense activity appears to be concentrated along the BFZ, although earthquake hypocenters are distributed throughout the study area and south of BFZ. Earthquakes occurred generally at shallow depths, in the upper 15 km of the crust, with magnitude that only in two events was larger than 7.0.

The Fig. 15a shows the focal mechanisms available in the literature (McKenzie, 1972; Taymaz et al., 1991, 2007; Sengor et al., 2005 with references), from which it is clear the dextral transcurrent strike-slip nature of the movement. A compressive component of the motion (deformation) is however observable along faults parallel or synthetic to NAFZ, whereas a normal-sinistral component is detectable along the antithetic fault systems (Kocygit et al. 2001; Taymaz & Tan 2001).

An approximately N-S trending cross-section was constructed along a transect crossing the study area by projecting the earthquake hypocenters and extending at depth the main

faults identified at surface, matching the faults with hypocenter clusterings (Fig. 15b). The Fig. 15b depicts a schematic representation of the hypothesized model; the reported crustal thicknesses are taken from the interpreted geoelectric cross-section by Kaya (2010) and the seismic profiles by Yolsal-Çevikbilen et al. (2012). The geometries assumed in our model are in agreement with the structures proposed by other authors in neighbouring areas (Andrieux et al., 1995; Kaya, 2010; Yildirim et al., 2011).

The resulting geometry is consistent with the interpretation of the NAFZ as a transpressional system, consisting of a crustal-scale flower structure, with faults that steepen and converge at depth. At depth the flower structure coincides with the boundary between the Anatolian microplate and the Eurasian plate (Fig. 15b).

The NAFZ developed along older reactivated structures, the Intrapontide Suture Zone represented by the accretionary complex created by closure of the Tethys Ocean and its branches (Şengör and Yılmaz, 1981; Göncüoğlu et al., 2008, 2012). The regional shear zones between AFZ and BFZ coincides with the main outcrops of the ophiolites and metamorphic units of Intrapontide Suture Zones (Fig. 2, 3 and 15). However some Intrapontide remnants crop out outside of the main shear zone, south of the Tosya area (Fig. 2). These outcrops can be interpreted as originated by south-vergence low-angle thrusts or as high-angle faults bounded blocks, in the NAFZ crustal-scale flower structure.

The available data do not allow us to hypothesize an extension of the fault inside the lithospheric mantle, and therefore remains the uncertainty of whether the fault is a plate boundary (Sengor, 1979; Barka 1996; Piper 1997; Stein 1997; Hubert Ferrari et al., 2002; Biryol et al., 2010) or an indent-linked strike-slip fault (Dewey & Sengor, 1979; Woodcock, 1986; Sylvester, 1988).

6. Conclusions

From the results of the geological-structural study which investigated the NAFZ in Central Anatolia (Kursunlu-Arac area), we can draw the following conclusions.

- This NAFZ sector is characterized by the development and polyphase evolution of two master faults, the Arac Fault Zone and the Bayramoren Fault Zone, overall trending parallel to the main shear direction, showing main dextral strike-slip displacement.
- The dextral movement along Arac and Bayramoren fault zones has created a 25 km wide dextral transpressional zone. Inside this zone, brittle deformation has been

partitioned roughly according to the Riedel theoretical model. Actually, the resulting strain partitioning is extremely more complex than predicted by theoretical models, with the combination of high-angle faults, low-angle thrust faults and folds with double vergence distributed along three main directions, coinciding with PDZ, R and R' directions of the models.

- Deformation partitioning developed pervasively during the NAFZ transpressional phase, so that flower structures commonly characterize deformation at the mesoscale. Therefore it is possible to hypothesize the whole NAFZ deformation zone in the Kursunlu-Arac area as a crustal scale positive flower structure.

The conclusions above emphasize that a careful structural study, including kinematic analysis, understanding of the geometric connections between regional structures and fault/fold relationships along principal, synthetic and antithetic faults, should be considered carefully in the future studies on deformation distribution in transpressional zones.

Acknowledgements

The authors gratefully acknowledge …… reviewers. This research benefits by grants from PRIN 2008 and PRIN 2010-11 projects (resp. M. Marroni) and from IGG-CNR.

References

Aksay A., Pehlivan Ş., Gedik I., Bilginer E., Duru M., Akbaş B. & Altun I. (2002) – Geological Map of Turkey (1:500.000 scale): sheet n.2 Zonguldak. General Directorate of Mineral Research and Exploration.

Allen CR. 1969. Active faulting in northern Turkey. Contrib. No. 1577, Div. Geol. Sci., Calif. Inst. Technol. 32 pp.

Altiner D., Kocygit A., Farinacci A., Nicosia U. & Conti M.A. (1991) – Jurassic-Lower Cretaceous stratigraphy and paleogeographic evolution of the southern part of NW Anatolia, Turkey. Geologica Romana, 27, 13-80.

Ambraseys NN. 1970. Some characteristic features of the North Anatolian Fault Zone. Tectonophysics 9:143–65

Andrieux J., Över S., Poisson A. & Bellier O. (1995) – The North Anatolian Fault Zone: distributed Neogene deformation in its northward convex part. Tectonophysics, 243, 135-154.

Armijo R, Meyer B, Hubert-Ferrari A, Barka A. 1999. Westward propagation of North Anatolian Fault into the Northern Aegean: timing and kinematics. Geology 27:267–70

Barka A. 1992. The North Anatolian Fault zone. Ann. Tecton. 6:164–195

Barka, A., 1996. Slip distribution along the North Anatolian Fault associated with the Large
Earthquakes of the Period 1939 to 1967, BSSA, 86, 1238-1254.

Barka A, Akyuz HS, Cohen HA, Watchorn F. 2000. Tectonic evolution of the Niksar and Ta¸sova-Erbaa pull-apart basins, North Anatolian Fault Zone: their significance for the motion of the Anatolian Block. Tectonophysics 322:243–64

Biryol B.C., Zandt G., Beck S.L., Ozacar A.A., Adiyaman H.E. & Gans C.R. (2010) – Shear wave splitting along a nascent plate boundary: the North Anatolian Fault Zone. Geophys. J. Int. 181, 1201-1213.

Bozkurt E. & Koçyiğit A. (1996). The Kazova basin: an active negative flower structure on the Almus Fault Zone, a splay fault system of the North Anatolian Fault Zone, Turkey. Tectonophysics 265:239–54.

de Leeuw, G.A.M., Hilton, D.R., Gulec, N., Mutlu, H., 2010. Regional and temporal variations $CO_2/^3He$, $^3He/^4He$ and $\delta^{13}C$ along the North Anatolian Fault Zone, Turkey. Applied Geochemistry 25, 524–539.

Casas, A.M., Gapais, D., Nalpas, T., Besnard, K., Román-Berdiel, T., 2001. Analogue models of transpressive systems. Journal of Structural Geology 23, 733–743.

Catanzariti, R., Ellero, A., Göncüoğlu, M.C., Marroni, M., Ottria, G., Pandolfi, L. in review, The Taraklı Flysch in the Boyalı area (Sakarya Terrane, Northern Turkey): Implications for the tectonic history of the Intrapontıde Suture Zone. CR Geosciences submitted

Delvaux, D., Sperner, B., 2003. Stress tensor inversion from fault kinematic indicators and focal mechanism data: the TENSOR program. In: New Insights into Structural Interpretation and Modelling (D. Nieuwland Ed.). Geological Society, London, Special Publications 212, 75-100.

Dewey JF, Sengor AMC. 1979. Aegean and surrounding regions: complex multiplate and continuum tectonics in a convergent zone. Geol. Soc. Am. Bull. 90:84–92

Dewey, J. F., M. R. Hempton, W. S. F. Kidd, F. Saroglu, and A. M. C. Sengor (1986). Shortening of continental lithosphere: The neotectonics of eastern Anatolia– a young collision zone, in Collosion Tectonics, edited by M. P. Coward and A. C. Ries, Geological Society Special Publications19, 3 –36.

Dewey JF, Holdsworth RE, Strachan RA (1998) Transpression and transtension zones. In: Holdsworth RE, Strachan RA, Dewey JF (eds) Continental transpressional and transtensional tectonics. Geological Society Special Publication, 135:1–14

Dooley T.P. & Schreurs G. (2012). Analogue modelling of intraplate strike-slip tectonics: A review and new experimental results. Tectonophysics, 574-575, 1-71.

Elmas A. & Yiğitbaş E. (2001) – Ophiolite emplacement by strike-slip tectonics between the Pontide Zone and the Sakarya Zone in northwestern Anatolia, Turkey. Int. J. Earth Sciences, 90, 257-269.

Görür, N., Monod, O., Okay, A.I., Şengör, A.M.C., Tüysüz, O., Yiğitbaş, E., Sakınç, M., & Akkök, R. (1997). Palaeogeographic and tectonic position of the Carboniferous rocks of the western Pontides (Turkey) in the frame of the Variscan belt. Bulletin de la Société Géologique de France, v. 168, p. 197–205.

Göncüoğlu, M.C., Gürsu, S., Tekin, U.K., Köksal, S., 2008. New data on the evolution of the Neotethyan oceanic branches in Turkey: Late Jurassic ridge spreading in the Intra-Pontide branch. Ofioliti 33, 153-164.

Göncüoğlu, M.C., Marroni, M., Sayit, K., Tekin, U. K., Ottria, G., Pandolfi, L, Ellero, A., 2012. The Aylı Dag ophiolite sequence (central-northern Turkey): A fragment of middle Jurassic oceanic lithosphere within the Intra-Pontide suture zone. Ofioliti, 37, 77-91.

Goncuoglu M.C., Marroni M., Pandolfi L., Ellero A., Ottria G., Catanzariti R., Tekin U.K., Sayit K. (2013 in press) - The geodynamic history of the Intrapontide Suture Zone: evidences from the Arkotdag mélange in Araç area, central Turkey. Journal of Asian Earth Science.

Gulec, N., Hilton, D.R., Mutlu, H., 2002. Heliumisotope variations in Turkey: relationship to tectonics, volcanism and recent seismic activities. Chemical Geology 187, 129–142.

Herece E, Akay E. 2003. Kuzey Anadolu Fayı (KAF) Atlası/Atlas of North Anatolian Fault (NAF). Maden Tetk. Arama Genel Mudurlugu, Ozel Yayın. Ser. 2, Ankara, [IV]+61 pp.+13 appendices as separate maps.

Hippolyte J.C., Müller C., Kaymakci N. & Sangu E. (2010). Dating of the Black sea basin: new nannoplankton ages from its inverted margin in the Central Pontides (Turkey). In Sosson M., Kaymacki N., Stephenson R., Bergerat A. & Starostenko V. (eds.) Sedimentary Basin Tectonics from the Black Sea and Caucasus to the Arabian Platform. Geological Society, London, Special Publications, 340, 113-136.

Holdsworth, R.E., Butler, C.A., Roberts, A.M., 1997. The recognition of reactivation during continental deformation. Journal of the Geological Society of London 154, 73±78.

Hubert-Ferrari, A., R. Armijo, G. King, B. Meyer, and A. Barka (2002). Morphology, displacement, and slip rates along the North Anatolian Fault, Turkey, J. Geophys. Res., 107(B10), 2235, doi:10.1029/2001JB000393.

Hubert-Ferrari A., King G., Manighetti I., Armijo R, Meyer B. and Tapponnier P. (2003) - Long-term elasticity in the continental lithosphere; modelling the Aden Ridge propagation and the Anatolian extrusion process. Geophys. J. Int. 153, 111–132.

International Seismological Centre. ISC Bulletin. http://www.isc.ac.uk/iscbulletin

Italiano F., Sasmaz A., Yuce G. & Okan O.O. (2013). Thermal fluids along the East Anatolian Fault Zone (EAFZ): Geochemical features and relationships with the tectonic setting. Chemical Geology 339, 103-114.

Jackson, J. A., and D. McKenzie (1988), The relationship between plate motions and seismic moment tensors, and the rates of active deformation in the Mediterranean and Middle East, Geophys. J., 93, 45– 73.

Jones RR, Tanner GPW (1995) Strain partitioning in transpression zones. J Struct Geol 17:793–802.

Kaya C. (2010). Deep crustal structure of northwestern part of Turkey. Tectonophysics, 489, 227-239.

Kaymakçı, N., Stanley, H.W., and Vandijk, P.M. (2003). Kinematic and structural development of the Çankırı Basin (Central Anatolia, Turkey): A paleostress inversion Study. Tectonophysics, v. 364, p. 85–113.

Keskin M., Genç Ş.C.. & Tüysüz O. (2008) - Petrology and geochemistry of post collisional Middle Eocene volcanic units in North-Central Turkey: Evidence for magma generation by slab breakoff following the closure of the Northern Neotethys Ocean. Lithos, 104, 267-305.

Ketin İ. 1948. Über die tektonisch-mechanischen Folgerungen aus den grossen anatolischen Erdbeben des letzten Dezenniums. Geol. Rund. 36:77–83

Ketin İ. 1957. Kuzey Anadolu Deprem Fayı.İTÜ Derg. 15:49–52

Kiratzi AA. 1993. A study of the active crustal deformation of the North and East Anatolian fault zones. Tectonophysics 225:191–203

Koçyiğit A, Rojay B, Cihan M, Özacar A. 2001. The June 6, 2000 Orta (Çankırı, Turkey) earthquake: sourced from a new antithetic sinistral strike-slip structure of the North Anatolian Fault system, the Dodurga Fault Zone. Turk. J. Earth Sci. 10:69–82

Kocyigit A, Yılmaz A, Adamia S, Kuloshvili S. 2001. Neotectonics of East Anatolian Plateau (Turkey) and Lesser Caucasus: implications for transition from thrusting to strike-slip faulting. Geodin. Acta 14:177–95

Le Pichon X, Sengor AMC, Demirbag E, Rangin C, Imren C, et al. 2001. The active Main Marmara Fault. Earth Planet. Sci. Lett. 192:595–616

Le Pichon X, Chamot-Rooke N, Rangin C, Sengor AMC. 2003. The North Anatolian Fault in the Sea of Marmara. J. Geophys. Res. 108(B4):2179

McClusky S, Balassanian S, Barka A, Demir C, Ergintav S, et al. 2000. Global Positioning System constraints on plate kinematics and dynamics in the eastern Mediterranean and Caucasus. J. Geophys. Res. 105:5695–719

McKenzie, D., 1972. Active tectonics of Mediterranean region, Geophys. J.R. astr. Soc., 30, 109–185.

McKenzie, D., The East Anatolian Fault: A major structure in eastern Turkey, Earth Planet Sci. Lett., 29, 189– 193, 1976.

Meade BJ, Hager BH, McClusky SC, Reilinger RE, Ergintav S, et al. 2002. Estimates of seismic potential in the Marmara Sea region from block models of secular deformation constrained by Global Positioning System measurements. Bull. Seismol. Soc. Am. 92:208– 15

Naylor, M.A., Mandl, G., Sijpesteijn, C.H.K., 1986. Fault geometries in basement-induced wrench faulting under different initial stress states. Journal of Structural Geology 8, 737–752.

Neugebauer J. (1995) – Structures and kinematics of the North Anatolian Fault zone, Adapazari-Bolu region, northwest Turkey. Tectonophysics, 243, 119-134.

Okay A. & Tüysüz O. (1999). Tethyan sutures of northern Turkey. In The Mediterranean Basins: Tertiary Extension within the Alpine Orogen, Geol. Soc. London, Spec. Publ. 156, ed. B Durand, L Jolivet, F Horvàth, M Séranne, pp. 475–515.

Okay Aİ, Demirbağ E., Kurt H., Okay N. & Kuşçu İ. (1999) – An active, deep marine strike-slip basin along the North Anatolian Fault in Turkey. Tectonics, 18, 129-147.

Okay Aİ, Kaşlılar-Özcan A., İmren C., Boztepe-Güney A., Demirbağ E. & Kuşçu İ. (2000). Active faults and evolving strike-slip basins in the Marmara Sea, northwest Turkey: a multichannel seismic reflection study. Tectonophysics, 321, 189-218.

Okay, Aİ. & Göncüoğlu, M.C. (2004). Karakaya Complex: A review of data and concepts: Turkish Journal of Earth Sciences, v. 13, p. 77–95.

Okay Aİ., Tüysüz O., Satur M., Özkan-Altiner S., Altiner D., Sherlock S. & Eren R.H. (2006). Cretaceous and Triassic subduction-accretion, high-pressure-low-temperature metamorphism, and continental growth in the Central Pontides, Turkey. GSA Bulletin, 118 (9/10), 1247-1269.

Oldow JS, Bally AW, Ave Lallemant HG (1990) Transpression, orogenic float and lithospheric balance. Geology 18:991–994.

Özcan E., Less G. & Kertész B. (2007). Late Ypresian to Middle Lutetian orthophragminid record from central and northern Turkey: taxonomy and remarks on zonal scheme. Turkish J. Earth Sci., 16, 281-318.

Ozden S., Over S., Kavak K.S. & Inal S.S. (2008) – Late Cenozoic stress states around the Bolu Basin along the North Anatolian Fault, NW Turkey. Journal of Geodynamics, 46, 48–62

Piper, J. D. A., Tatar, O., and Gursoy, H., 1997. Deformational behavior of continental lithosphere deduced from block rotations across the North Anatolian fault zone in Turkey, Earth and Planetary Sci. Letters, 150, 191-203.

Piper J.D.A., Gürsoy H., Tatar O., Beck M.E., Rao A., Koçbulut F. & Mesci B.L. (2010). Distributed neotectonic deformation in the Anatolides of Turkey: A palaeomagnetic analysis. Tectonophysics. 488: 31-50.

Ramsay JC (1967) Folding and fracturing of rocks. Mc-Graw-Hill, New York, pp 1–568.

Reilinger RE, McCLusky SC, Oral MB, King RW, Toksoz MN. 1997. Global Positioning System measurements of present-day crustal movements in the Arabia-Africa-Eurasia plate collision zone. J. Geophys. Res. 102:9983–99.

Reilinger, R., et al. (2006), GPS constraints on continental deformation in the Africa-Arabia-Eurasia continental collision zone and implications for the dynamics of plate interactions, J. Geophys. Res., 111, B05411, doi:10.1029/2005JB004051.

Robertson, A.H.F., Ustaömer, T., 2004. Tectonic evolution of the Intra-Pontide suture zone in the Armutlu Peninsula, NW Turkey. Tectonophysics, 381: 175-209.

Rotstein, Y., 1984. Counterclockwise rotation of the Anatolian Block. Tectonophysics, 108, 71-91.

Rotstein, Y., and A. L. Kafka, Seismotectonics of the southern boundary of Anatolia, eastern Mediterranean region: Subduction, collision, and arc jumping, Journ. Geophys. Res., 87, 7694–7706, 1982.

Sanderson D. & Marchini R.D. (1984). Transpression. J. Struct. Geol., 6, 449-458.

Sayit K. & Goncuoglu M.C. (2013). Geodynamic evolution of the Karakaya Mélange Complex, Turkey: A review of geological and petrological constraints. Journal of Geodynamics, 65, 56-65.

Schreurs, G., Colletta, B., 2003. Analogue modelling of continental transpression. In: Schellart, W.P., Passchier, C. (Eds.), Analogue Modelling of Large-scale Tectonic Processes. Journal of the Virtual Explorer 7, 103–114.

Sengor AMC. 1979. The North Anatolian Transform Fault: its age, offset and tectonic significance. J. Geol. Soc. London 136:269–82

Sengor AMC. 1990. Plate tectonics and orogenic research after 25 years: A Tethyan perspective. Earth Sci. Rev. 27:1–201

Sengor, A. M. C., and W. S. F. Kidd (1979). Post-collisional tectonics of the Turkish-Iranian. Plateau and a comparison with Tibet, Tectonophysics, 55, 361– 376.

Sengor AMC, Yılmaz Y. (1981). Tethyan evolution of Turkey: a plate tectonic approach. Tectonophysics 75:181–241

Sengor AMC, Gorur N, Saroglu F. 1985. Strikeslip faulting and related basin formation in zones of tectonic escape: Turkey as a case study. In Strike-slip Deformation, Basin Formation, and Sedimentation, Soc. Econ. Paleontol. Miner. Spec. Publ. 37 (in honor of J.C. Crowell), ed. KT Biddle, N Christie-Blick, pp. 227–64

Sengor AMC, Ozeren S, Genc¸ T, Zor E. 2003. East Anatolian high plateau as a mantle-supported, north-south shortened domal structure. Geophys. Res. Lett. 30: 8045

Sengor, A.M.C., Tuysuz, O., Imren, C., Sakınç, M., Eyidogan, H., Gorur, N., Le Pichon, X., Rangin, C., 2005. The north Anatolian fault: a new look. Annual Review of Earth and Planetary Sciences 33, 37–112.

Stein, R. S., Barka, A., and Dieterich, J. H., 1997. Progressive failure on the North Anatolian fault since 1939 by earthquake stress triggering, Geophys. J. Int., 128, 594-604.

Sunal, G. & Tüysüz, O. 2002. Paleo-stress analyses of Tertiary post-collisional structures in the Western Pontides: northern Turkey. Geological Magazine 139, 343–359.

Tankut A., Wilson M. & Yihunie T. (1998) - Geochemistry and tectonic setting of Tertiary volcanism in the Güvem area, Anatolia, Turkey. Journal of Volcanology and Geothermal research, 85, 285-301.

Taymaz, T., Jackson, J.&McKenzie, D., 1991. Active Tectonics of the North and Central Aegean Sea, Geophys. J. Int., 106(2), 433–490.

Taymaz T. & Tan O. 2001. Source parameters of June 6, 2000 Orta-Çankırı and December 15, 2000 Sultandağı-Akşehir earthquakes (Mw=6.0) obtained from inversion of teleseismic body wave forms. In Taymaz (ed.): ”Symposia on Seismotectonics of the North–Western Anatolia—Aegean and Recent Turkish Earthquakes: Scientific Activities 2001”, 96–107.

Taymaz, T., Wright, T., Yolsal, S., Tan, O., Fielding, E. & Seyitoglu, G., 2007. Source characteristics of June 6, 2000 Orta-Çankırı (Central Turkey) Earthquake: a synthesis of seismological, geological and geodetic (InSAR) observations, and internal deformation of Anatolia Plate, Geol. Soc. London Spec. Pub., 291, 259–290, doi:10.1144/SP291.12.

Tchalenko, J.S., 1970. Similarities between shear zones of different magnitudes. Geological Society of America Bulletin 81, 1625–1640.

Tikoff B. & Teyssier C. (1994). Strain modelling of displacement-field partitioning in transpressional orogens. J. Struct. Geol., 16, 1575-1588.

Tokay, M., 1973. Geological observations on them North Anatolian Fault Zone between Gerede and Ilgaz. Proceed. North Anatolian Fault and Earthquakes Symposium, Ankara. The Mineral Research and Exploration Publication, p. 12-29.

Turkelli, N., et al. (2003). Seismogenic zones in Eastern Turkey, Geophys. Res. Lett., 30(24), 8039, doi:10.1029/ 2003GL018023.

Tüysüz O. (1999). Geology of the Cretaceous sedimentary basins of the Western Pontides: Geological Journal, v. 34, p. 75–93.

Uğuz M.F., Sevin M. & Duru M. (2002) – Geological Map of Turkey (1:500.000 scale): sheet n.3 Sinop. General Directorate of Mineral Research and Exploration.

Uysal, I.T., Mutlu, H., Altunel, E., Karabacak, V., Golding, S.D., 2006. Clay mineralogical and isotopic (K–Ar, $\delta^{18}O$, δD) constraints on the evolution of the North Anatolian Fault Zone, Turkey. Earth and Planetary Science Letters 243, 181–194.

Westaway R. (1994) – Present-day kinematics of the Middle east and eastern Mediterranean. Journal of Geophysical Research, 99, 12,071 – 12,090.

White, S.H., Bretan, P.G., Rutter, E.H., 1986. Fault-zone reactivation: kinematics and mechanisms. Philosophical Transactions of the Royal Society of London A317, 81-97.

Wilcox, R.E., Harding, T.P., Seely, D.R., 1973. Basic wrench tectonics. American Association of Petroleum Geologists Bulletin 57, 74–96.

Yaltırak, C., Alpar, B., Yüce, H., 1998. Tectonic elements controlling the evolution of the Gulf of Saros (Northeastern Aegean Sea). Tectonophysics 300, 227-248.

Yaltırak C. & Alpar B. (2002). Kinematics and evolution of the northern branch of the North Anatolian Fault (Ganos Fault) between the Sea of Marmara and the Gulf of Saros. Mar. Geol. 190:351–66.

Yiğitibaş E., Elmas A., Sefunç A. & Özer N. (2004) – Major neotectonic features of eastern marmara region, Turkey: development of the Adapazari-Karasu corridor and its tectonic significance. Geol. J. 39: 179–198.

Yildirim, C., T. F. Schildgen, H. Echtler, D. Melnick, and M. R. Strecker (2011). Late Neogene and active orogenic uplift in the Central Pontides associated with the North Anatolian Fault: Implications for the northern margin of the Central Anatolian Plateau, Turkey, Tectonics, 30, TC5005.

Yılmaz O. & Boztuğ, D. (1986). Kastamonu granitoid belt of northern Turkey: First arc plutonism product related to the subduction of the Paleo-Tethys: Geology, v. 14, p. 179–183.

Yılmaz, Y., Genc, SC., Yigitbas, E., Bozcu, M. and Yılmaz, K. 1995 Geological evolution of the late Mesozoic continental margin of Northwestern Anatolia. Tectonophysics 243, 155-171

Yılmaz Y, Genc S¸C, Gurer F, Bozcu M, Yılmaz K, et al. 2002. When did the western Anatolian grabens begin to develop? In Tectonics and Magmatism in Turkey and Surrounding Area, ed. E Bozkurt, JAWinchester, JDA Piper, pp. 353–84. Geol. Soc. London, Spec. Publ. No. 173.

Yolsal-Çevikbilen S., Biryol C.B., Beck S., Zandt G., Taymaz T., Adıyaman H.E. & Özacar A. A. (2012). 3-D crustal structure along the North Anatolian Fault Zone in north-central Anatolia revealed by local earthquake tomography. Geophys. J. Int., 188, 819-849.

Zattin M., Okay A.I. & Cavazza W., 2005. Fission-track evidence for late Oligocene and mid-Miocene activity along the North Anatolian Fault in southwestern Thrace. Terra Nova 17, 95–101.

Zattin M., Cavazza W., Okay A.I., Federici I., Fellin M.G., Pignalosa A. & Reiners P. (2010) - A precursor of the North Anatolian Fault in the Marmara Sea region. Journal of Asian Earth Sciences 39 (3), 97-108.

Captions

Fig. 1. Tectonic framework of the Anatolian block and surrounding regions (simplified from Barka, 1992). Yellow arrows show directions of current relative plate motion. Solid lines are strike-slip faults, lines with triangles are thrust faults. The offshore tectonic lineaments are indicated in white.

Fig. 2. a) Major tectonic units and terranes in Turkey (revised from Okay and Tüysüz, 1999). b) Simplified tectonic map of the Central Pontides in the Eskipazar – Tosya area, where the NAFZ is more or less coincident with the Intra-Pontide Suture Zone. AFZ: Arac Fault Zone; BFZ: Bayramoren Fault Zone.

Fig. 3. a) Structural geological map of the study area. AFZ: Arac Fault Zone; BFZ: Bayramoren Fault Zone. b) Geological cross sections. See Fig. 3a for acronyms and locations.

Fig. 4. Statistical analysis of structural data from the fault systems of the Bayramoren Fault Zone. Rose diagrams showing dip (a) and strike (b) of the fault systems. In stereogram (c) traces of strike-slip faults with observed slip lines and slip senses are shown (equal-area stereographic projections, lower emisphere). The principal stress axes (σ_1, σ_2, σ_3) and type of stress tensor were obtained using Win_TENSOR software (Delvaux and Spencer, 2003).

Fig. 5. Panoramic view of the Bayramoren Fault Zone (BFZ). In the picture kilometric size fault-bounded blocks are particularly evident. The photo is taken looking towards SE.

Fig. 6. Geometrical and kinematic features along Bayramoren Fault Zone. a) Detail of a fault plane on Upper Jurassic-Lower Cretaceous limestone of the Sakarya terrane, bearing oblique slickenlines with a dextral sense of movement. The direction of the red arrow corresponds to the movement of the missing block. b) Pluridecametric exposure of a positive flower structure developed in the Upper Jurassic-Lower Cretaceous limestone of the Sakarya terrane. Stereographic projection (Schmidt net, lower emisphere), of the structure is showed, with the traces of fault planes, observed slip lines and slip senses. c) Low-angle thrust surface associated to high-angle faults developed in the Eocene

deposits. Stereographic projection (Schmidt net, lower emisphere), of the structure is showed, with the traces of fault planes, observed slip lines and slip senses. d) Decametre-scale NW-vergent fold developed in the Upper Jurassic-Lower Cretaceous limestone of the Sakarya terrane. In stereogram (Schmidt net, lower emisphere) circles are bedding, triangles are measured fold axes and square is calculated fold axes.

Fig. 7. Aerial view redraws from Google Map of Arac Fault Zone (AFZ). BFZ: Bayramoren Fault Zone; SAT: Sakarya terrane; IPS: Intrapontide Suture Zone; IZT: Istanbul Zonguldak terrane.

Fig. 8. Statistical analysis of structural data from the fault systems of the Arac Fault Zone. Rose diagrams showing dip (a) and strike (b) of the fault systems. In stereogram (c) traces of strike-slip faults with observed slip lines and slip senses are shown (equal-area stereographic projections, lower emisphere). The principal stress axes (σ_1, σ_2, σ_3) and type of stress tensor were obtained using Win_TENSOR software (Delvaux and Spencer, 2003).

Fig. 9. Schematic 3D sketch of the geometrics and kinematics features of the AFZ juxtaposing the Eocene deposits with the Tarakli Flysch. a) and c) are outcrops coincident with a xz plane of finite strain ellipsoid, showing shear planes with S-C type structures, typical of compressional kinematics. The same structures observed along sections coincident with xy plane of the finite strain ellipsoid (b), are characterized by a dextral strike-slip kinematic.

Fig. 10. North-vergent thrust surface belonging to AFZ cutting the Eocene deposits.

Fig. 11. Geometrical and kinematic features of the Boyali Area. a) Type 3 interference structure (Ramsay, 1967) between D1 and D2 folds developed in Tarakli Flysch. In stereogram (Schmidt net, lower emisphere) D1 (circles) and D2 (squares) fold axes are plotted. b) High-angle dextral strike-slip fault developed in Tarakli Flysch. Stereographic projection (Schmidt net, lower emisphere), of the structure is showed, with the traces of fault planes, observed slip lines and slip senses. c) Detail of the strike-slip fault in Fig. 11b, with striated surface showing a dextral sense of movement. The direction of the red arrow corresponds to the movement of the missing block. d) Fault plane bearing multiple

generations of slickenlines represented by calcite fibres, suggesting a polyphasic activity along the fault plane, with the last phase characterized by an oblique-normal component of movement. The direction of the red arrow corresponds to the movement of the missing block. e) Low-angle shear zone with the development of S-C structure. Stereographic projection (Schmidt net, lower emisphere), of the structure is showed, with the traces of fault planes, observed slip lines and slip senses. f) Mesoscale positive flower structure developed in Tarakli Flysch. Stereographic projection (Schmidt net, lower emisphere), of the structure is showed, with the traces of fault planes, observed slip lines and slip senses.

Fig. 12. Statistical analysis of structural data from the fault systems of the Boyali Area. Rose diagrams showing dip (a) and strike (b) of the fault systems. In stereogram (c) traces of strike-slip faults with observed slip lines and slip senses are shown (equal-area stereographic projections, lower emisphere). The principal stress axes (σ_1, σ_2, σ_3) and type of stress tensor were obtained using Win_TENSOR software (Delvaux and Spencer, 2003).

Fig. 13. Statistical analysis of the overall structural data from the Kursunlu-Arac area (Schmidt net, lower emisphere). a) Contour plot of the fault planes. b) Contour plot of the thrust surfaces. c) Contour plot of the fold axes.

Fig. 14. Schematic sketch of the main structural features of the Kursunlu-Arac area, between the Arac Fault Zone (AFZ) and the Bayramoren Fault Zone (BFZ). A strain ellipse is shown in the box to highlight the expected structural character in a zone of dextral shear (after Wilcox et al., 1973). The structures identified in the field has been referred to the structure systems predicted by the theory assigning the same colour.

Fig. 15. a) Distribution of epicentres of earthquakes with M≥3 that occurred since 1900 in an area between Karabuk to the West and Osmancik to the East (ISC Bulletin). Fault plane solutions available in literature for this area are also shown (McKenzie, 1972; Taymaz et al., 1991, 2007; Sengor et al., 2005 with references). b) Conceptual model for the NAFZ hypothesized as a crustal-scale flower structure.

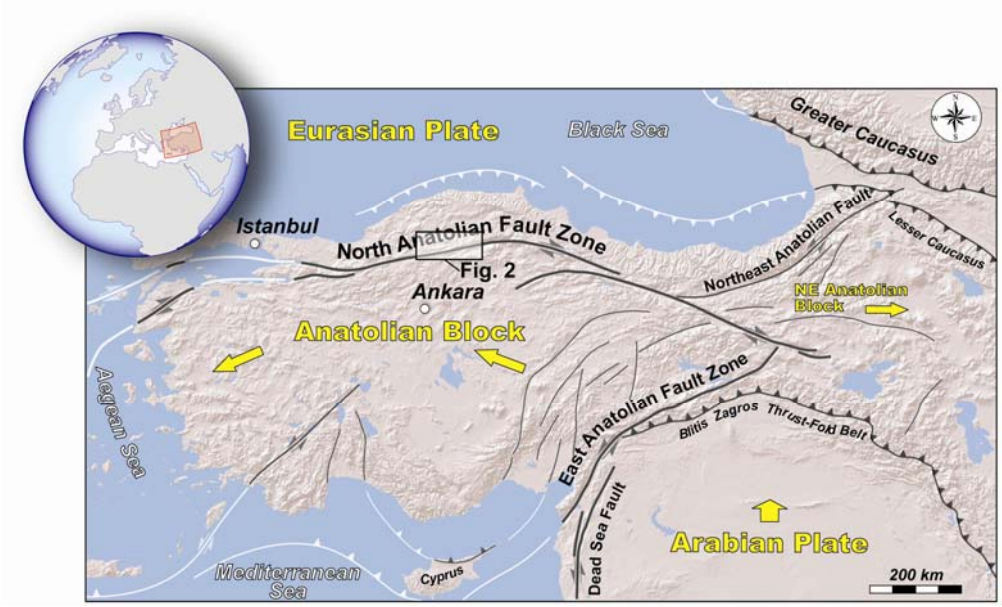

Fig. 1. Tectonic framework of the Anatolian block and surrounding regions (simplified from Barka, 1992). Yellow arrows show directions of current relative plate motion. Solid lines are strike-slip faults, lines with triangles are thrust faults. The offshore tectonic lineaments are indicated in white.

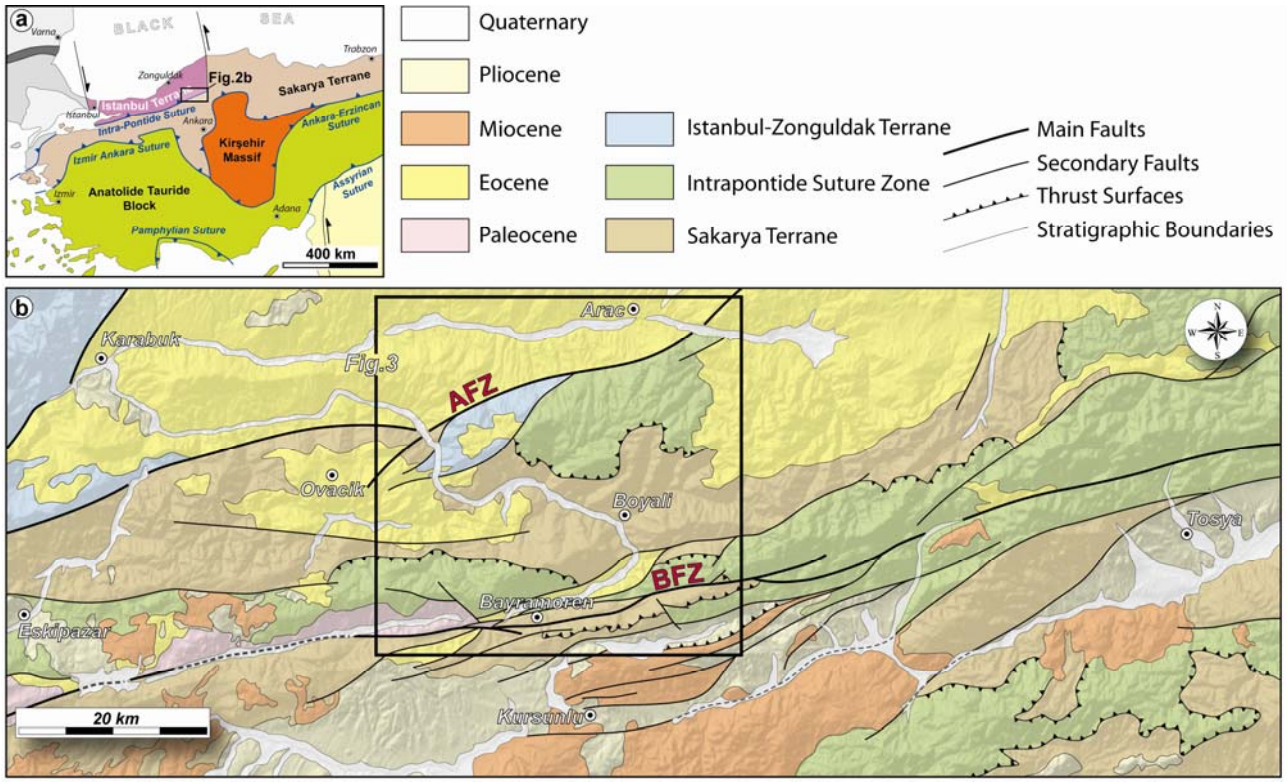

Fig. 2. a) Major tectonic units and terranes in Turkey (revised from Okay and Tüysüz, 1999). b) Simplified tectonic map of the Central Pontides in the Eskipazar – Tosya area, where the NAFZ is more or less coincident with the Intra-Pontide Suture Zone. AFZ: Arac Fault Zone; BFZ: Bayramoren Fault Zone.

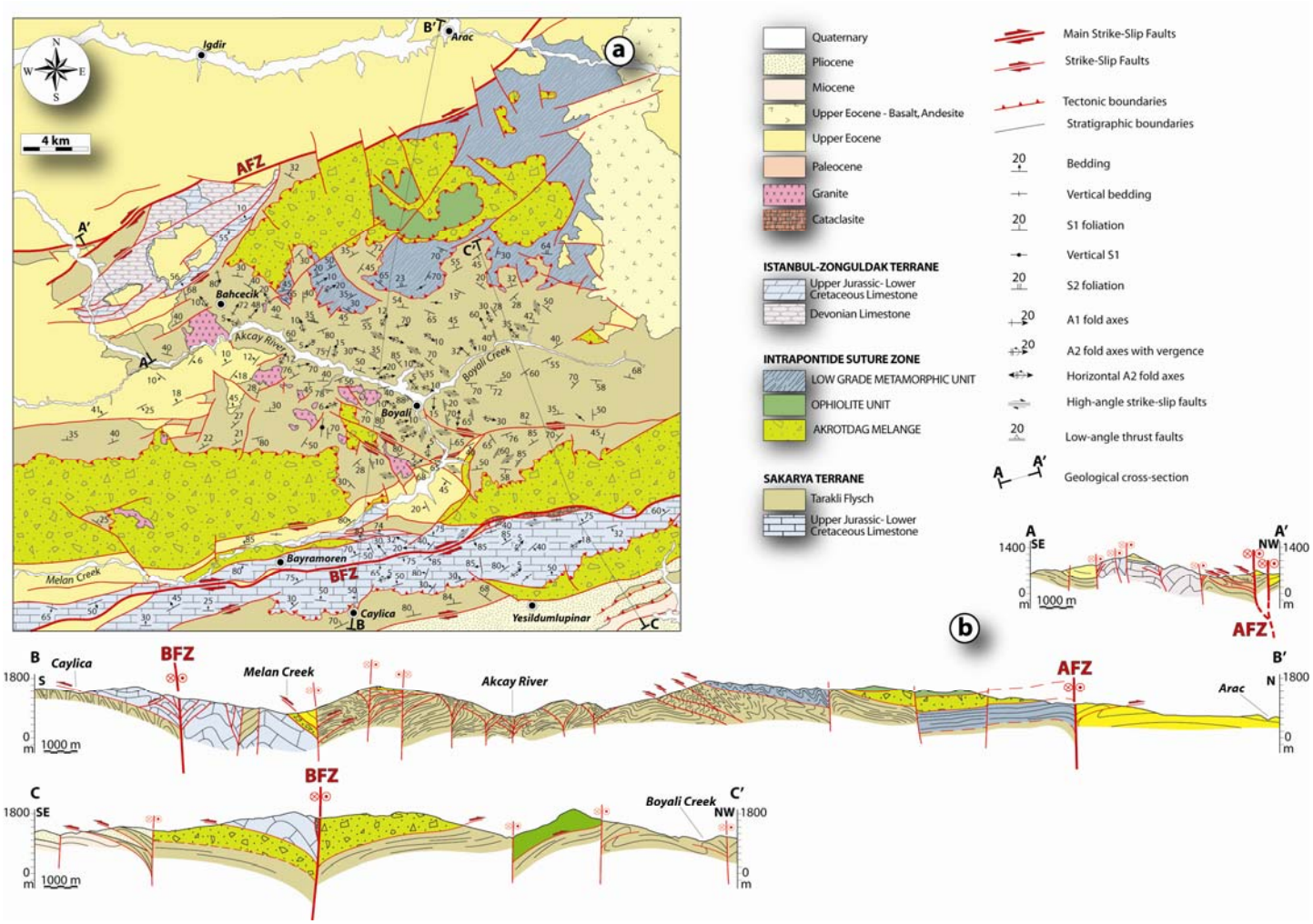

Fig. 3. a) Structural geological map of the Bayramoren-Arac area. AFZ: Arac Fault Zone; BFZ: Bayramoren Fault Zone. b) Geological cross section across the study area. See Fig. 3a for acronyms and locations.

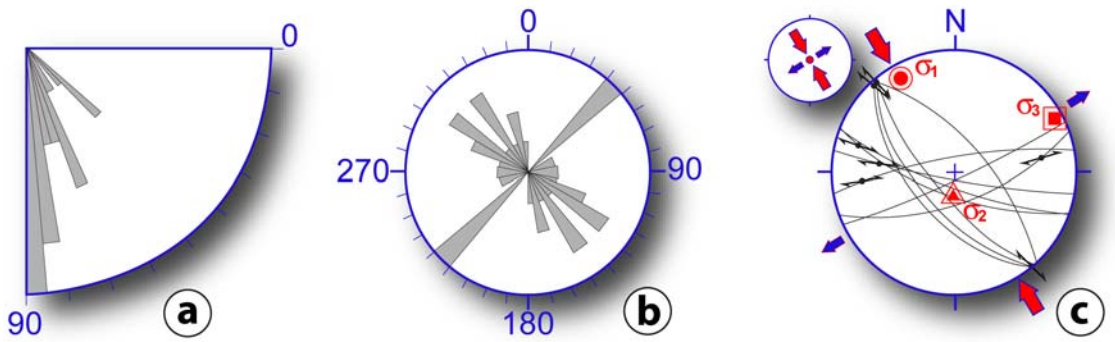

Fig. 4. Statistical analysis of structural data from the fault systems of the Bayramoren Fault Zone. Rose diagrams showing dip (a) and strike (b) of the fault systems. In stereogram (c) traces of strike-slip faults with observed slip lines and slip senses are shown (equal-area stereographic projections, lower emisphere). The principal stress axes (σ_1, σ_2, σ_3) and type of stress tensor were obtained using Win_TENSOR software (Delvaux and Spencer, 2003).

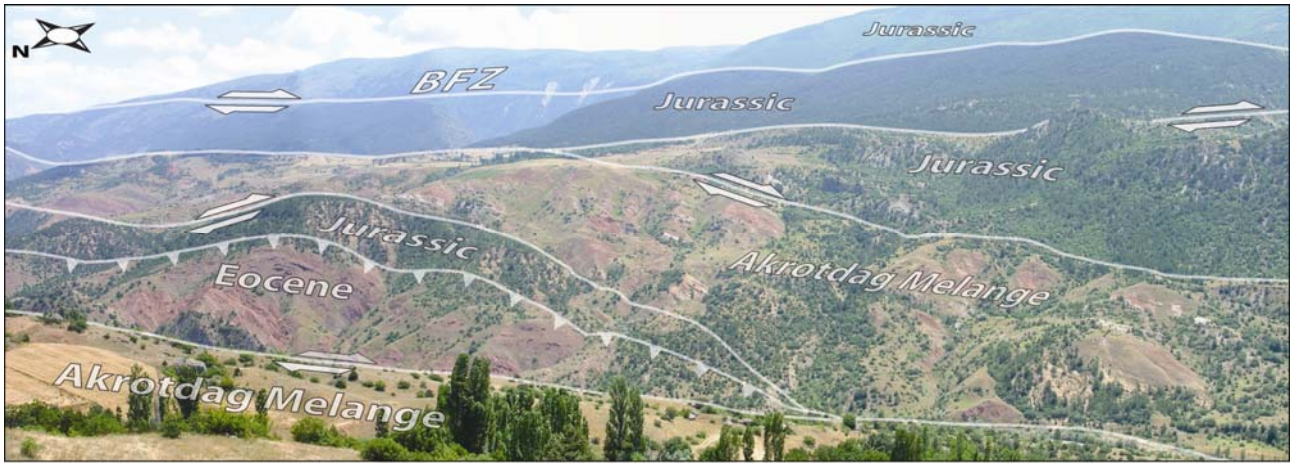

Fig. 5. Panoramic view of the Bayramoren Fault Zone (BFZ). In the picture kilometric size fault-bounded blocks are particularly evident. The photo is taken looking towards SE.

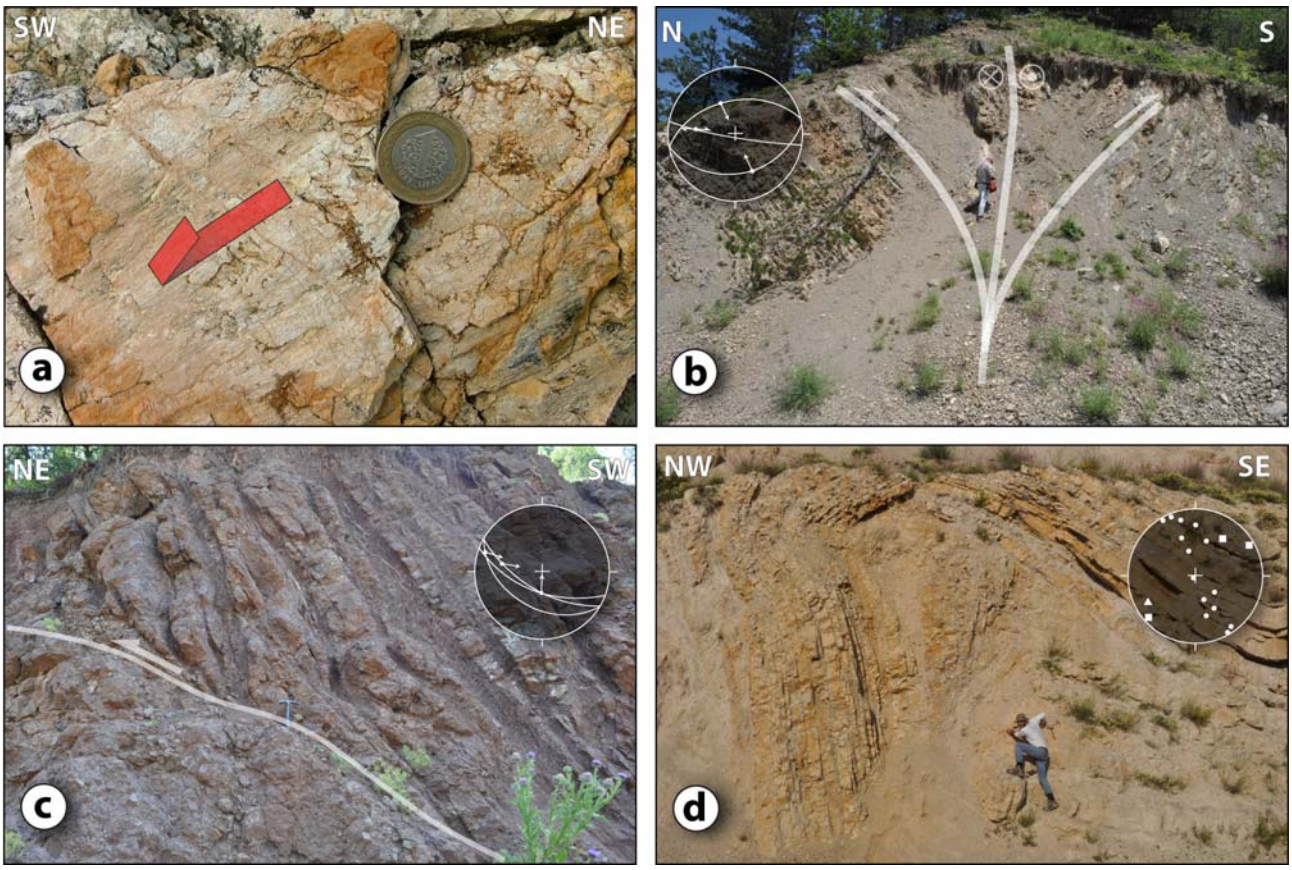

Fig. 6. Geometrical and kinematic features along Bayramoren Fault Zone. a) Detail of a fault plane on Upper Jurassic-Lower Cretaceous limestone of the Sakarya terrane, bearing oblique slickenlines with a dextral sense of movement. The direction of the red arrow corresponds to the movement of the missing block. b) Pluridecametric exposure of a positive flower structure developed in the Upper Jurassic-Lower Cretaceous limestone of the Sakarya terrane. Stereographic projection (Schmidt net, lower emisphere), of the structure is showed, with the traces of fault planes, observed slip lines and slip senses. c) Low-angle thrust surface associated to high-angle faults developed in the Eocene deposits. Stereographic projection (Schmidt net, lower emisphere) of the structure is showed, with the traces of fault planes, observed slip lines and slip senses. d) Decametre-scale NW-vergent fold developed in the Upper Jurassic-Lower Cretaceous limestone of the Sakarya terrane. In stereogram (Schmidt net, lower emisphere) circles are bedding poles, squares are measured fold axes and triangle is calculated fold axis.

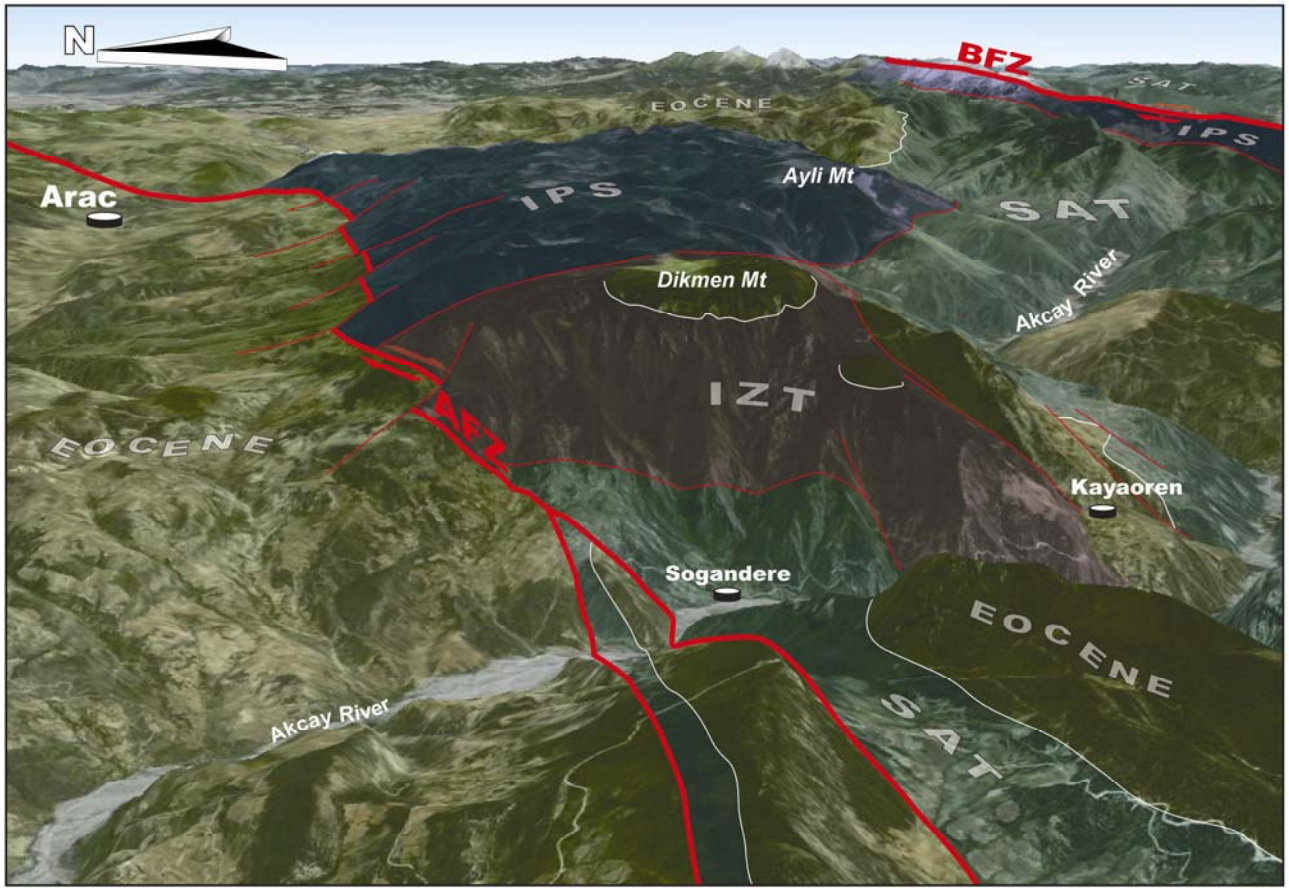

Fig. 7. Aerial view redraws from Google Map of Arac Fault Zone (AFZ). BFZ: Bayramoren Fault Zone; SAT: Sakarya terrane; IPS: Intrapontide Suture Zone; IZT: Istanbul Zonguldak terrane.

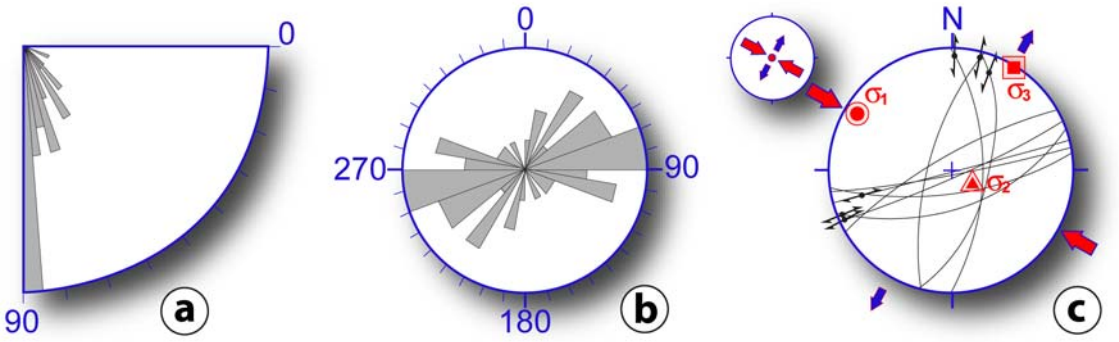

Fig. 8. Statistical analysis of structural data from the fault systems of the Arac Fault Zone. Rose diagrams showing dip (a) and strike (b) of the fault systems. In stereogram (c) traces of strike-slip faults with observed slip lines and slip senses are shown (equal-area stereographic projections, lower emisphere). The principal stress axes (σ_1, σ_2, σ_3) and type of stress tensor were obtained using Win_TENSOR software (Delvaux and Spencer, 2003).

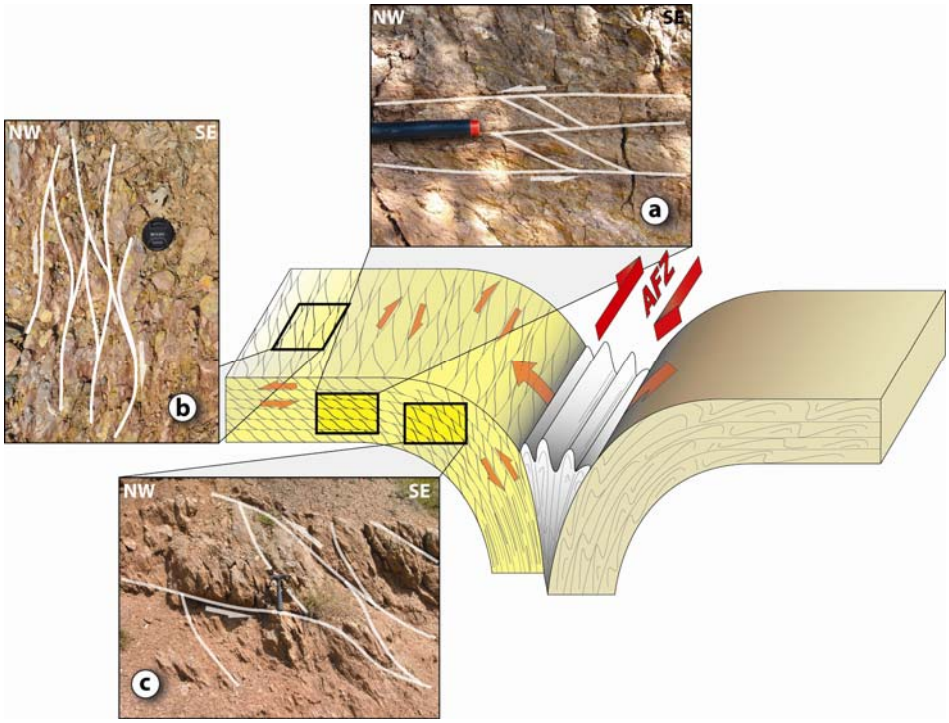

Fig. 9. Schematic 3D sketch of the geometrics and kinematics features of the AFZ juxtaposing the Eocene deposits with the Tarakli Flysch. a) and c) are outcrops coincident with a xz plane of finite strain ellipsoid, showing shear planes with S-C type structures, typical of compressional kinematics. The same structures observed along sections coincident with xy plane of the finite strain ellipsoid (b), are characterized by a dextral strike-slip kinematic.

Fig. 10. North-vergent thrust surface belonging to AFZ cutting the Eocene deposits.

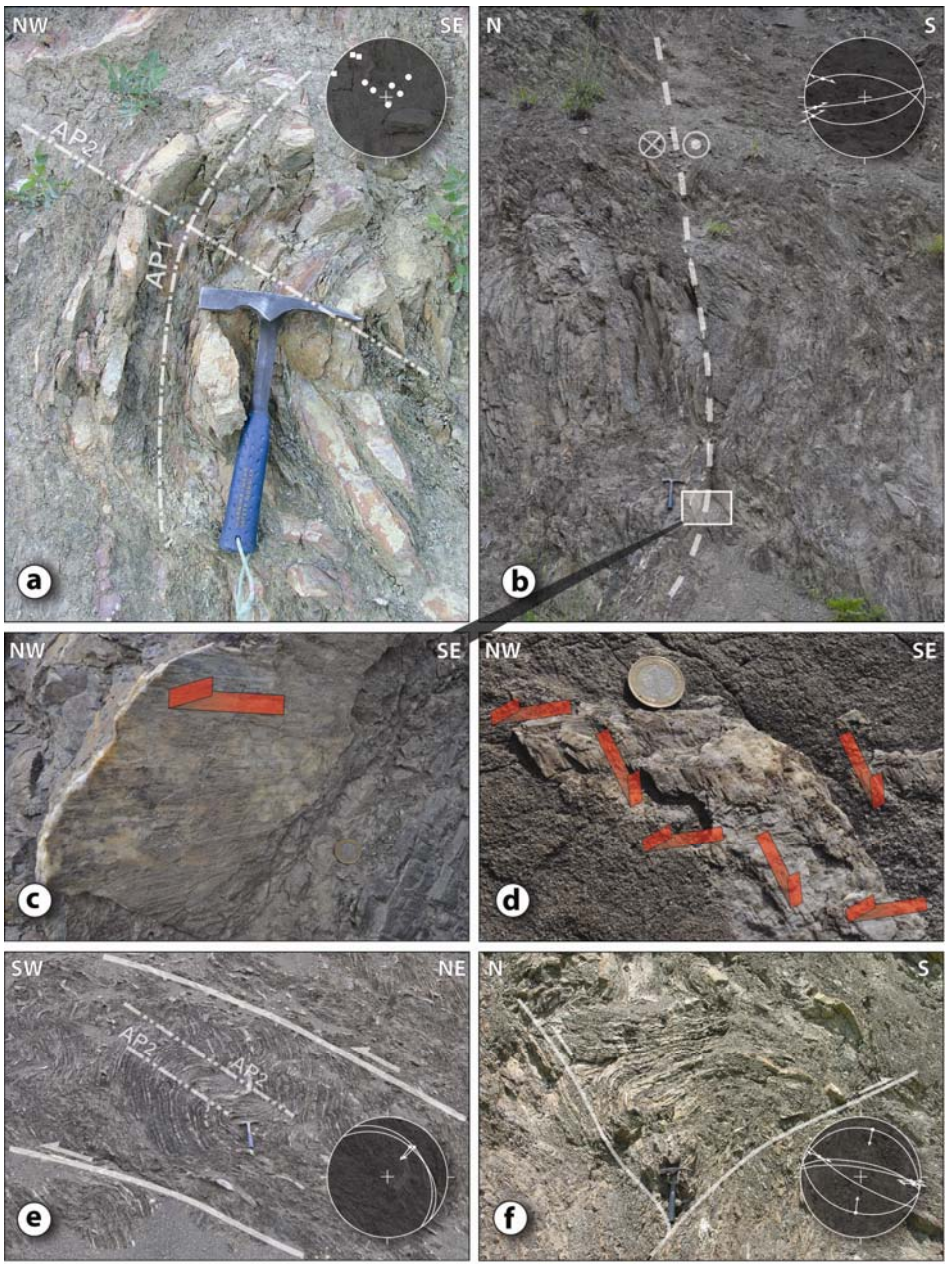

Fig. 11. Geometrical and kinematic features of the Boyali Area. a) Type 3 interference structure (Ramsay, 1967) between D1 and D2 folds developed in Tarakli Flysch. In stereogram (Schmidt net, lower emisphere) D1 (circles) and D2 (squares) fold axes are plotted. b) High-angle dextral strike-slip fault developed in Tarakli Flysch. Stereographic projection (Schmidt net, lower emisphere), of the structure is showed, with the traces of fault planes, observed slip lines and slip senses. c) Detail of the strike-slip fault in Fig. 11b, with striated surface showing a dextral sense of movement. The direction of the red arrow corresponds to the movement of the missing block. d) Fault plane bearing multiple generations of slickenlines represented by calcite fibres, suggesting a polyphasic activity along the fault plane, with the last phase characterized by an oblique-normal component of movement. The direction of the red arrow corresponds to the movement of the missing block. e) Low-angle shear zone with the development of S-C structure. Stereographic projection (Schmidt net, lower emisphere), of the structure is showed, with the traces of fault planes, observed slip lines and slip senses. f) Mesoscale positive flower structure developed in Tarakli Flysch. Stereographic projection (Schmidt net, lower emisphere), of the structure is showed, with the traces of fault planes, observed slip lines and slip senses.

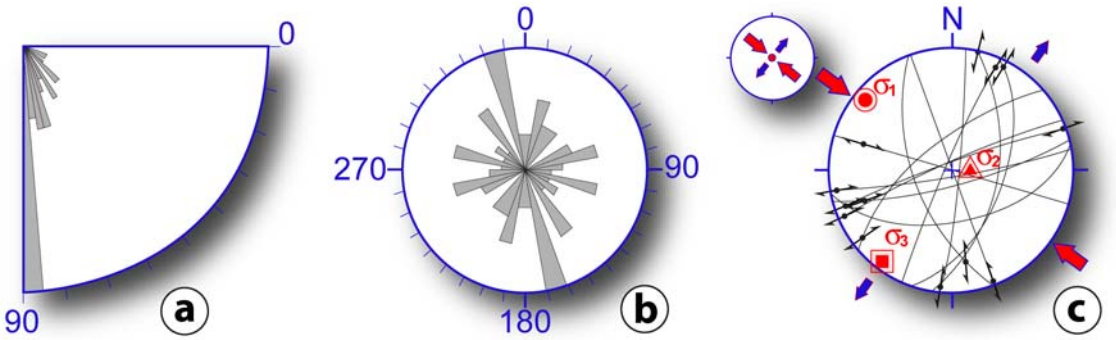

Fig. 12. Statistical analysis of structural data from the fault systems of the Boyali area. Rose diagrams showing dip (a) and strike (b) of the fault systems. In stereogram (c) traces of strike-slip faults with observed slip lines and slip senses are shown (equal-area stereographic projections, lower emisphere). The principal stress axes (σ_1, σ_2, σ_3) and type of stress tensor were obtained using Win_TENSOR software (Delvaux and Spencer, 2003).

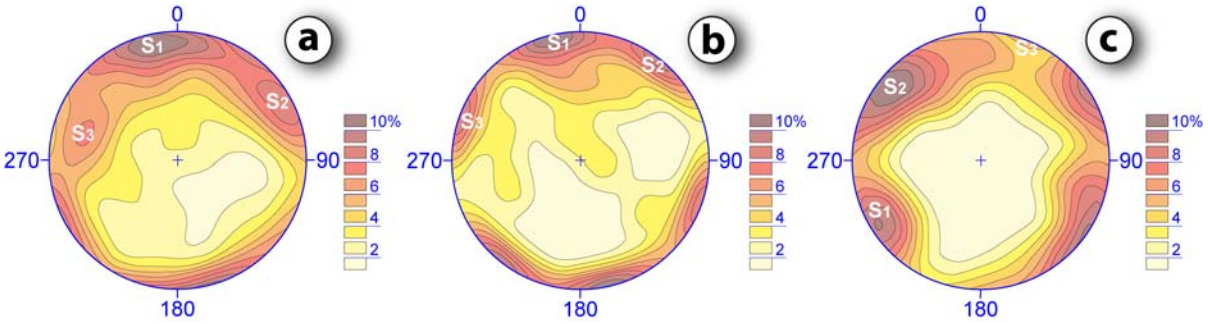

Fig. 13. Statistical analysis of the overall structural data from the Kursunlu-Arac area (Schmidt net, lower emisphere). a) Contour plot of the fault planes. b) Contour plot of the thrust surfaces. c) Contour plot of the fold axes.

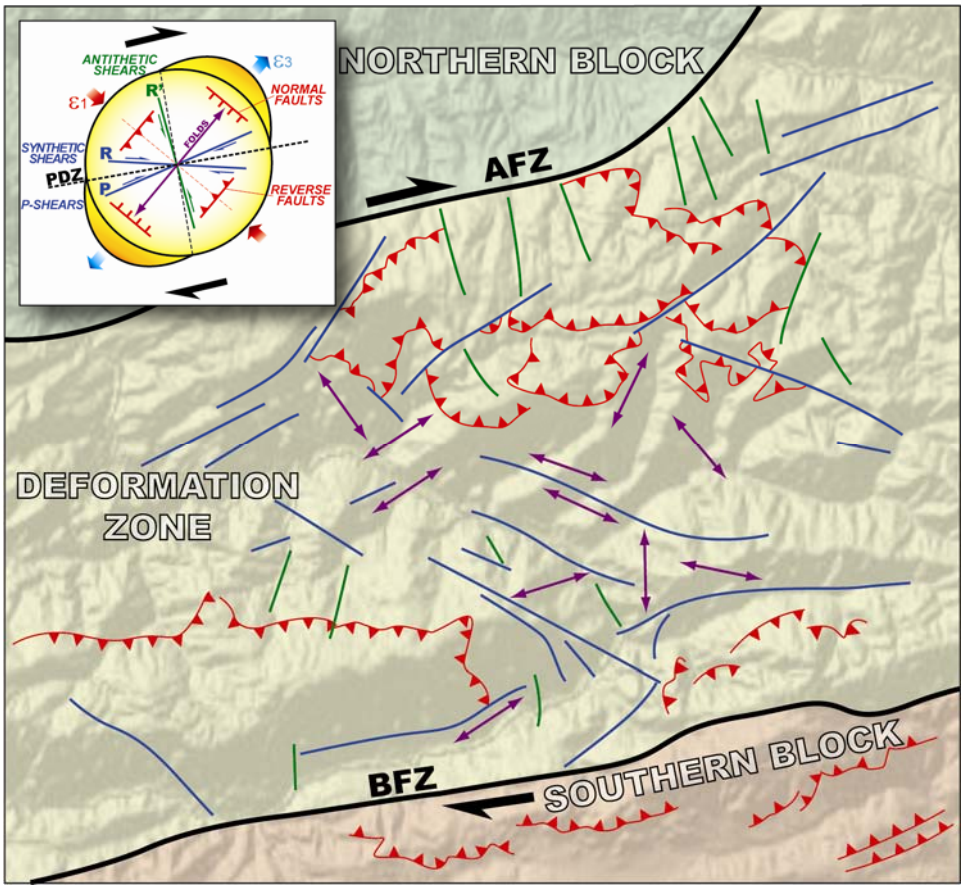

Fig. 14. Schematic sketch of the main structural features of the Kursunlu-Arac area, between the Arac Fault Zone (AFZ) and the Bayramoren Fault Zone (BFZ). A strain ellipse is shown in the box to highlight the expected structural character in a zone of dextral shear (after Wilcox et al., 1973). The different structures identified in the field has been referred to the structure systems predicted by the theory assigning them the same colour.

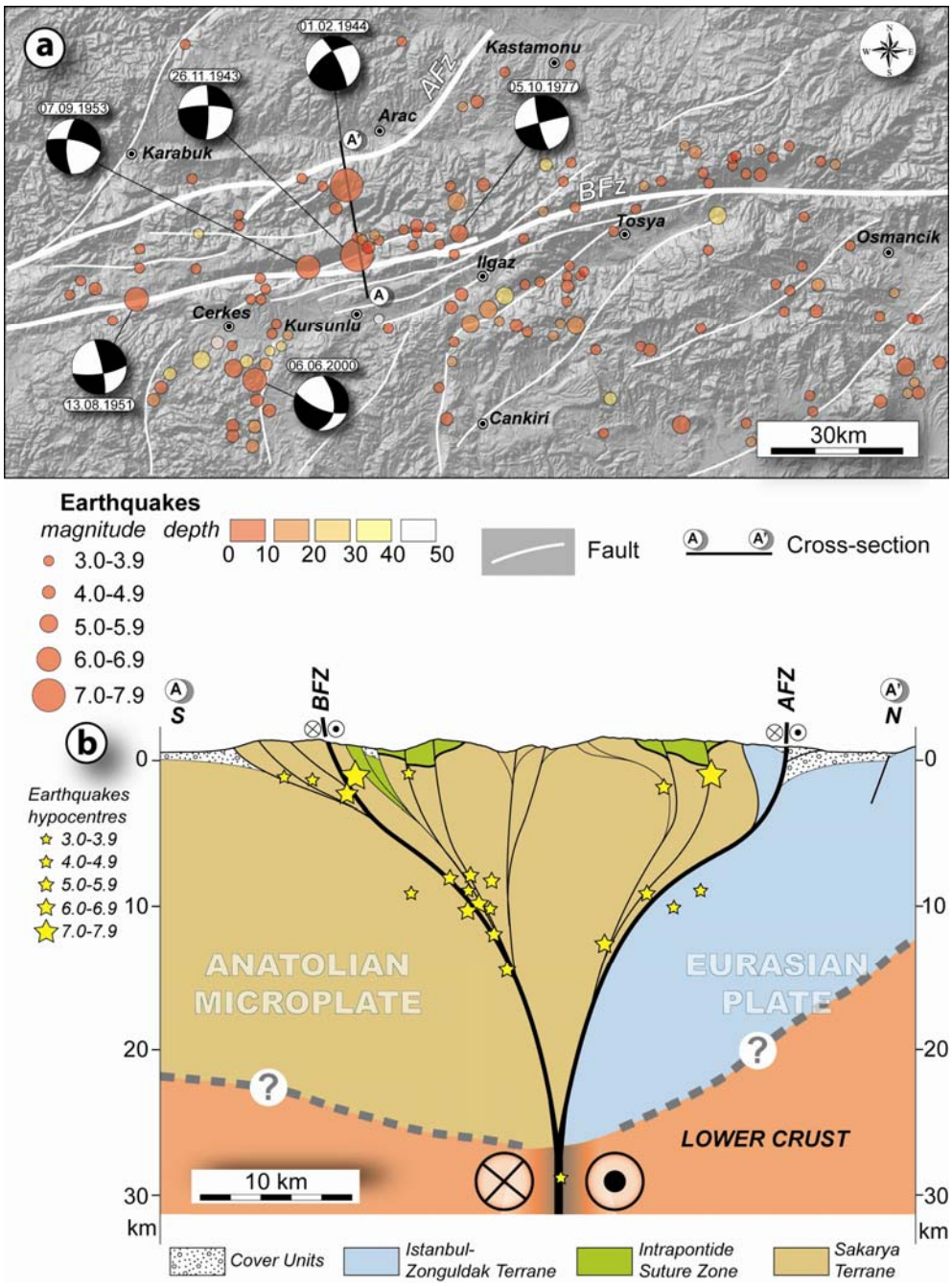

Fig. 15. a) Distribution of epicentres of earthquakes with M≥3 that occurred since 1900 in an area between Karabuk to the West and Osmancik to the East (International Seismological Centre. ISC Bulletin). Fault plane solutions available in literature for this area are also shown (McKenzie, 1972; Taymaz et al., 1991, 2007; Sengor et al., 2005 with references). b) Conceptual model for the NAFZ hypothesized as a crustal-scale flower structure.